found in the NTD, which comprises two His and two Cys residues (HHCC motif). HHCC motif is a zinc-binding motif that contributes to the multimerization and catalytic function of IN. In contrast, CTD is the least conserved of the domains amongst retroviral INs but makes nonspecific contacts with DNA [1]. Retroviral integration catalyzed by IN proceeds in well-characterized 3′-processing and strand transfer steps; these chemical reactions are reproducible *in vitro* with recombinant IN and DNA substrates, demonstrating that IN alone is sufficient to carry out the DNA breakage and joining reactions [1,2].

IN is expressed as a C-terminal part of the Gag-Pol polyprotein from integrated provirus and incorporated into the virion during the late phase of infection. After assembly, viral protease (PR) cleaves the Gag-Pol precursor as well as the Gag precursor to yield a mature virion [3]. In retroviral genomic RNA, Gag and Pol proteins are encoded by overlapping open reading frames (ORF), and Gag-Pol is generated by either a ribosomal frameshifting during translation of *gag* or a read-through suppression on the *gag* termination codon. These translation mechanisms result in intracellular synthesis of Gag-Pol proteins at 10- to 20-fold-lower than Gag proteins [3]. Although the synthesis of Gag suffices to produce virus-like particles, incorporation and processing of Gag-Pol is integral to the morphogenesis of virions [3,4], indicating an important role of the Gag-Pol precursor in the formation of infectious virions during retroviral replication.

As mentioned above, the enzymatic activities of retroviral IN in integration reactions have been clearly defined by numerous *in vitro* biochemical studies using recombinant IN protein and oligonucleotide DNA substrates [1]. However, many mutation studies on the *IN* gene of infectious HIV-1 molecular clones have demonstrated that the IN gene also has roles on multiple steps of virus replication in addition to integration. This pleiotropic effect of IN is characterized by a defect in uncoating, reverse transcription, nuclear import, viral gene expression, virion precursor protein processing, and virion morphology [5–11]; however, the mechanism for the pleiotropic effect of IN gene is still poorly understood.

A number of cellular proteins have been identified as binding partners for human immunodeficiency virus type 1 (HIV-1) IN [2,12] and Moloney murine leukemia virus (MoMLV) IN [13]. In the case of HIV-1, some of the cellular interactors have been reported to assist in facilitating the integration reaction in virus-infected cells [2]. In particular, lens epithelium-derived growth factor (LEDGF) is a critical factor that acts as a chromosomal receptor that tethers IN and viral DNA to host DNA, thereby promoting integration during HIV-1 infection [12]. On the other hand, several lines of evidence demonstrate that other cellular partners for IN such as integrase interactor 1 (INI1), Gemin2, von Hippel-Lindau binding protein 1, transportin 3, and nucleoporin 153 appear to be implicated in steps other than the integration process during HIV-1 infection [2,14–18]. Overexpression or small interfering RNA (siRNA)-mediated depletion of these factors influence stages of reverse transcription, nuclear import, gene expression, and virion production during HIV-1 replication cycle [14,15,17–19]. Although exact roles of the IN-binding proteins in retroviral infection remain to be completely elucidated, these data suggest that a protein–protein interaction between retroviral IN and its cellular partner would be a primary basis for the pleiotropic effects that have been found from studies with IN mutant viruses.

In the present study, we identified Huwe1 (HECT, UBA, and WWE domain containing 1), a HECT (homologous to E6-AP carboxyl terminus)-domain ubiquitin ligase, as a novel cellular interactor of HIV-1 IN. The interaction was mediated through the CCD of HIV-1 IN and a wide-range region of Huwe1. Interestingly, Huwe1 also interacted with the IN portion of the HIV-1 Gag-Pol precursor protein. In addition, our study showed that Huwe1 appeared to modulate HIV-1 infectivity in virus producer cells, which influenced the step of proviral DNA synthesis in the next round of infection.

2. Materials and methods

2.1. Cells

NIH3T3 cells, 293T cells, and TZM-bl cells (a HeLa cell line expressing CD4, CXCR4, and CCR5 and containing an integrated *lacZ* reporter gene under the control of an HIV-1 LTR) [20] were maintained in Dulbecco's modified Eagle medium supplemented with 10% fetal calf serum (FCS) and antibiotics. MT-4 cells were maintained in RPMI 1640 supplemented with 10% FCS and antibiotics.

2.2. Construction of expression vectors for MoMLV and HIV-1 IN

To generate a plasmid expressing TAP tag-fused MoMLV IN (pCeMM-GS-MoMLV IN), MoMLV IN cDNA was amplified by PCR from pNCA [21] and inserted into pCeMM-NTAP(GS)-Gw [22]. For construction of a plasmid expressing C-terminal HA-tagged MoMLV IN, the MoMLV IN cDNA was cloned into pCTAP-A (Stratagene) and, subsequently, an intron sequence of human *β-globin* gene [23] and HA tag sequence were inserted into the vector. The plasmid expressing C-terminal V5-tagged HIV-1 IN and its domain mutants were described previously [23].

2.3. Tandem affinity purification and mass spectrometry analysis

NIH3T3 cells (7×10^5 cells) were transfected with 50 μg of pCeMM-GS-MoMLV-IN or empty vector by the calcium phosphate method, collected 48 h after transfection, and lysed in TAP lysis buffer (20 mM HEPES, pH 7.5, 5 mM $MgCl_2$, 150 mM KCl, 0.2% NP-40, 1 mM DTT, protease inhibitors). Cell debris was removed by centrifugation, and 200 μl of IgG Sepharose 6 Fast Flow (GE Healthcare) was added to lysate and incubated at 4 °C for 2 h. Beads were washed with lysis buffer twice and, subsequently, with TAP washing buffer (50 mM Tris–HCl, pH 8.0, 150 mM NaCl, 0.5 mM EDTA, 0.2% NP-40, 1 mM DTT) once. Proteins were eluted in 300 μl of TAP washing buffer containing 30 U of tobacco etch virus (TEV) protease (AcTEV, Invitrogen) at 4 °C. The sample was then

incubated with 100 μl of Streptavidin Sepharose High Performance (GE Healthcare) at 4 °C for 2 h. The beads were washed with TAP washing buffer containing protease inhibitors five times. Finally, protein complexes were eluted in 2 ml of TAP washing buffer containing 5 mM biotin (Pierce) and protease inhibitors, and concentrated. Mass spectrometric identification of proteins was performed as previously described [24].

2.4. Construction of expression vectors for Huwe1

To generate an ORF of murine Huwe1 (13137 bp), cDNA covering amino acid position 1–3567 (fragment 1), 3214–7178 (fragment 2), 5487–8907 (fragment 3), 8531–10850 (fragment 4), and 10732–13137 (fragment 5) were amplified by RT-PCR from total the RNA of NIH3T3 cell and subcloned into pFLAG-CMV-2 (Sigma). Fragments 2–5 were excised from each plasmid by digestion with appropriate restriction enzymes and sequentially inserted into pFLAG-CMV-2 encoding fragment 1. For truncation mutants, Huwe1 cDNA containing position 2394–3617 was obtained from a plasmid encoding fragments 1–4 and cloned into the pFLAG-CMV-2. Similarly, cDNA positions 4005–4378 (HECT) was excised from a plasmid encoding fragment 5 and cloned into the pFLAG-CMV-2. Vectors encoding fragments 1 and 2 were used for expression of Huwe1 position 1–1072 and 1072–2394, respectively.

2.5. Immunoprecipitation assay

293T cells were transfected with a plasmid expressing either HA-tagged MoMLV IN or V5-tagged HIV-1 IN by the calcium phosphate method. Cells were collected at 48 h after transfection and lysed in TAP lysis buffer. After centrifugation, supernatant was incubated with 10 μg of anti-α-tubulin mouse monoclonal IgG (DM1A, Sigma) or anti-Huwe1 rabbit polyclonal IgG (Novus Biologicals) in presence of 20 μl of Protein G Sepharose Fast Flow (GE Healthcare) for 4 h. Beads were then washed with TAP lysis buffer 3 times. In additional immunoprecipitation assay, FLAG-tagged Huwe1 was co-expressed with V5-tagged HIV-1 IN in 293T cells, and subjected to immunoprecipitation assay using 5 μg of anti-FLAG mouse monoclonal IgG (M2, Sigma).

2.6. Western blotting analysis

Samples were lysed in SDS buffer [25], resolved by SDS-PAGE gels, and transferred to Immobilion P Transfer Membrane (Millipore). Primary antibodies used were anti-α-tubulin mouse monoclonal IgG (DM1A, Sigma), anti-Huwe1 rabbit polyclonal IgG (Novus Biologicals), anti-V5 mouse monoclonal IgG (Invitrogen), and anti-FLAG mouse monoclonal IgG (M2, Invitrogen). Horseradish peroxidase (HRP)-conjugated anti-mouse or anti-rabbit IgG (Cell Signaling) was used as a secondary antibody. Detection of HA-tagged protein was carried out using HRP-conjugated anti-HA rat monoclonal IgG (3F10, Roche). For immunoprecipitation analysis, TrueBlot ULTRA HRP anti-mouse or anti-rabbit IgG (eBioscience) was used as a secondary antibody.

2.7. Generation of Huwe1 knockdown cell line and HIV-1 infection experiments

By using the BLOCK-iT Pol II miR RNAi Expression Kit (Invitrogen), synthesized oligonucleotide containing microRNA (miRNA) sequence against human Huwe1 ORF (nucleotide position 10854–10874) or no specific gene (control miRNA [Invitrogen]) was cloned into a lentiviral vector, CSII-CMV-MCS-GATEWAY-IRES-hrGFP, in which the multiple cloning site of CSII-CMV-MCS-IRES-hrGFP [26] had been replaced with a Gateway cloning system reading frame cassette. Infectious lentiviral vectors pseudotyped with vesicular stomatitis virus G (VSV-G) were produced from 293T cells [25]. MT-4 cells were exposed to the lentiviral vectors and enriched for hrGFP positive cells using the FACSAria cell sorting system (BD Bioscience).

Preparation of virus stocks of HIV-1_{NL4-3} and a HIV-1-based vector bearing a luciferase gene (HIV-Luc), and the determination of $p24^{CA}$ concentration in virus solutions and the 50% tissue culture infectious dose ($TCID_{50}$) of HIV-1_{NL4-3} stock were performed as described previously [27,28].

In single-round infection experiments, 3×10^5 Huwe1 knockdown or control MT-4 cells were exposed to HIV-Luc containing 5 ng of $p24^{CA}$ at 37 °C for 2 h and cultured after washing twice. Cells were harvested at 48 h post-infection and subjected to a luciferase activity assay [27]. To measure the level of viral DNA synthesis, HIV-1_{NL4-3} containing 100 ng of $p24^{CA}$ were added to 1×10^6 cells, and incubated at 37 °C for 2 h. After three times washing, cells were cultured in fresh medium. Total DNA was isolated 24 h after infection and subjected to quantitative PCR with HIV Tat/Rev specific primers [29].

To analyze HIV-1 production from virus-infected cells, 3×10^5 Huwe1 knockdown or control MT-4 cells were infected with HIV-1_{NL4-3} at a MOI of 0.001 at 37 °C for 2 h. Cells were washed twice and cultured with 1.5 ml of fresh medium. Culture supernatant was harvested at 3 days after infection and 100 μl of the virus solution was added to 1×10^5 TZM-bl cells. β-galactosidase activity in the TZM-bl cells was measured 48 h after infection [30] and normalized for $p24^{CA}$ concentration in culture supernatant of MT-4 cells.

2.8. Electron microscopy analysis

HIV-1-infected cells were fixed with 2% glutaraldehyde in 0.05 M cacodylate buffer, pH 7.2 at 4 °C for 90 min. Fixed cells were washed six times with the same buffer, further fixed with 2% osmium tetroxide in the same buffer at 4 °C for 90 min, contrast-enhanced with 1% tannic acid (Mallinckrodt) in same buffer, treated with 1% sodium sulfate in the same buffer, and dehydrated in a graded ethanol series. The samples were then embedded in Plain Resin (Nisshin EM, Japan). Ultrathin sections made with an ultramicrotome (Sorvall MT-5000, Du Pont) were doubly-stained with uranyl acetate and lead citrate, and observed under a transmission electron microscope (H-7650, Hitachi, Japan).

2.9. Quantification of HIV-1 DNA

Virus solution (100 μl) derived from HIV-1-infected Huwe1 knockdown and control cells were added to 1×10^6 MT-4 cells, and incubated at 37 °C for 2 h. After washing twice, cells were cultured in fresh medium and harvested at 3, 6, and 24 h post-infection. Total DNA was purified using DNeasy Blood & Tissue Kit (Qiagen). Quantitative PCR for RT products and semiquantitative *Alu*-LTR PCR for integrated DNA were performed as described previously [31]. Heat-inactivated (65 °C, 30 min) virus was used as a negative control for infection.

2.10. Assay for HIV-1 Gag-Pol protein

An HIV-1 molecular clone expressing HA-tagged Gag-Pol was generated by the deletion of frameshift signal and the in-frame insertion of the HA tag sequence into the C-terminus of the *pol* gene of pNL4-3 bearing an inactive form of PR (Haraguchi and Morikawa, unpublished) [32]. Similar molecular clone expressing HA-tagged Gag-Pol/ΔIN was created by the addition of an HA tag at the C-terminus of RT and the insertion of a premature termination codon at the junction of RT-IN (Haraguchi and Morikawa, unpublished). FLAG-tagged Huwe1 and HA-tagged Gag-Pol were co-expressed in 293T cells, and cell lysate was subjected to immunoprecipitation using an anti-FLAG antibody.

2.11. Statistical analysis

Student's *t* test was used to determine statistical significance. *P* values lower than 0.05 were considered significant.

3. Results

3.1. Identification of new cellular interactors of retroviral IN

In order to identify novel cellular proteins that interact with retroviral IN, we employed a tandem affinity purification (TAP) procedure. TAP is a generic two-step affinity purification protocol for the isolation of TAP tag-fused proteins together with associated proteins under physiological conditions [22]. In this study, the TAP tag consisted of two IgG binding units and a streptavidin-binding peptide, which were separated by a TEV protease cleavage site [22]. N-terminal TAP tag-fused MoMLV IN was expressed transiently in NIH3T3 cells and recovered from cell extracts by two sequential purification steps [22]. Purified proteins were visualized by silver staining after SDS-PAGE. As shown in Fig. 1A, TAP-tagged MoMLV IN (lane 2), but not the TAP tag alone (lane 3), specifically co-purified with a 55 kDa and a >200 kDa proteins. Mass spectrometry analysis identified the 55 kDa band as a mixture of α- and β-tubulins, which exhibit similar molecular weight, and the >200 kDa band as

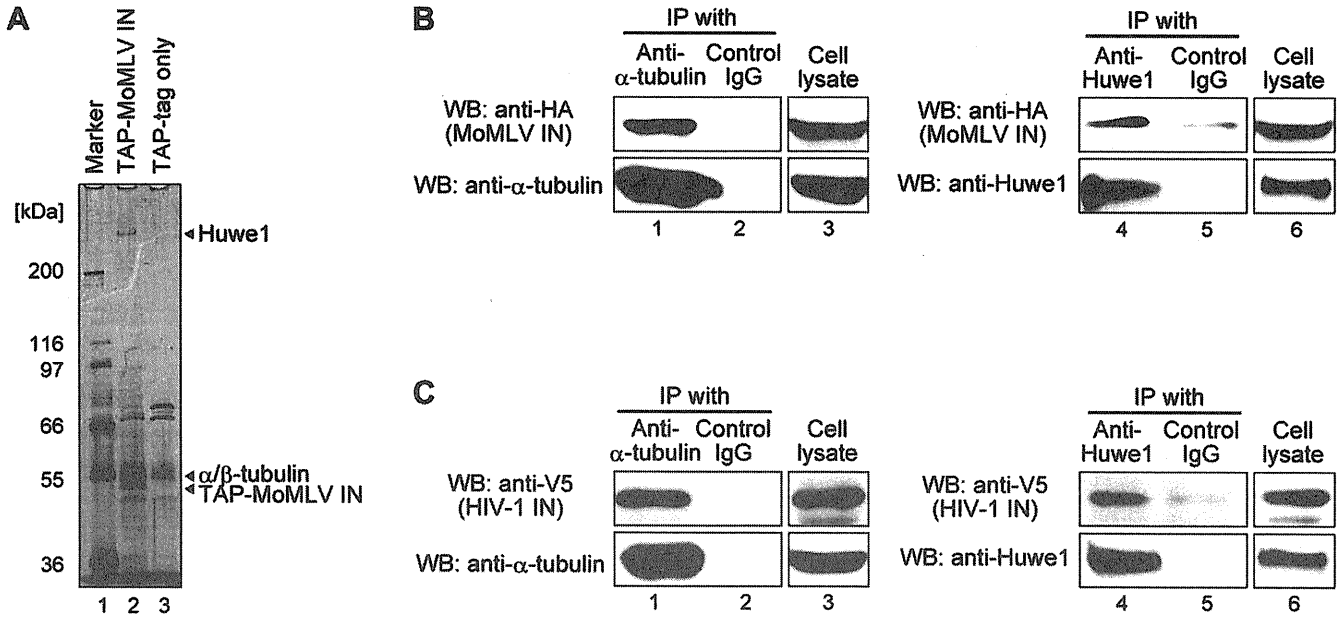

Fig. 1. Identification of tubulin and Huwe1 as cellular interactors of retroviral INs. (A) Tandem affinity purification for MoMLV IN. TAP tag-fused MoMLV IN (lane 2) was expressed in NIH3T3 cells, and protein complexes containing the TAP tag-fused IN were purified from cytoplasmic extract by two-step affinity purification procedure using IgG Sepharose and streptavidin Sepharose beads. Proteins were visualized by silver staining on a 10–20% SDS-PAGE gel, excised from the gel, and analyzed by MALDI-TOF/MS. As a control experiment, TAP tag was expressed and subjected to the tandem affinity purification (lane 3). Lane 1 shows molecular weight marker. (B and C) Interactions of endogenous α-tubulin and Huwe1 with MoMLV and HIV-1 IN. HA-tagged MoMLV IN (B) or V5-tagged HIV-1 IN (C) was expressed in 293T cells and co-immunoprecipitated (IP) with anti-α-tubulin (lane 1), anti-Huwe1 (lane 4), and control (lanes 2 and 5) antibodies. MoMLV IN and HIV-1 IN in the immunoprecipitates were detected by western blotting analysis (WB) using anti-HA (B) and anti-V5 antibodies (C), respectively.

Huwe1 [33] (Fig. 1A). We then confirmed the association by expression of HA-tagged MoMLV IN and subsequent co-immunoprecipitation with an anti-α-tubulin or an anti-Huwe1 antibody. Western blotting of the precipitates revealed that HA-tagged MoMLV IN was recovered by anti-α-tubulin and anti-Huwe1 antibodies (Fig. 1B, lanes 1 and 4), but not by control IgG (Fig. 1B, lanes 2 and 5), indicating specific binding of MoMLV IN to α-tubulin and Huwe1.

We next tested whether tubulin and Huwe1 bind to HIV-1 IN as well. To examine the binding, C-terminal V5-tagged HIV-1 IN was expressed transiently in 293T cells and subjected to co-immunoprecipitation assay using anti-α-tubulin and anti-Huwe1 antibodies. Western blotting analysis of the immunoprecipitates showed that endogenous α-tubulin and Huwe1 also interact with HIV-1 IN (Fig. 1C, lanes 1 and 4). It should be noted that, even when the lysates of MoMLV and HIV-1 IN expressing cells were treated with nucleases, interactions of the IN with α-tubulin and Huwe1 were not disrupted (data not shown), indicating that these interactions were not mediated through nucleic acids. Therefore, tubulin and Huwe1 were identified as the cellular interactors common to both MoMLV and HIV-1 IN.

3.2. Interaction domains between HIV-1 IN and Huwe1

Amongst the cellular proteins identified by our TAP procedure, Huwe1 is a novel IN-binding host protein, whereas tubulin has been reported to interact with HIV-1 IN [2]. Thus, we focused on the interaction between HIV-1 IN and Huwe1. To map the binding domain of IN, a series of V5-tagged HIV-1 IN containing truncated domain mutants were co-expressed with FLAG-tagged Huwe1 in 293T cells, and co-immunoprecipitation using an anti-FLAG antibody was performed. As in the case of the immunoprecipitation for endogenous Huwe1 (Fig. 1C), V5-tagged HIV-1 IN was associated with the FLAG-tagged Huwe1 (Fig. 2A, lane 2). A parallel co-immunoprecipitation assay using IN truncation mutants showed that the CCD of HIV-1 IN (Fig. 2A, lane 6), but not the NTD or CTD (Fig. 2A, lanes 4 and 8), was found to be sufficient for the interaction with Huwe1.

We next determined which region of Huwe1 is involved in the interaction with HIV-1 IN CCD. Analysis of the amino acid sequences have revealed that Huwe1 possesses several recognizable domains; ARLD (Armadillo [ARM] repeat like domain) 1 and 2 in the N-terminus, UBA (ubiquitin-associated), WWE, and well-conserved BH3 domains in the middle, and a HECT domain in the C-terminus (Fig. 2B) [34,35]. To understand the interaction region in Huwe1, we constructed plasmids expressing FLAG-tagged Huwe1 mutants encompassing ARLD1/2 (1–1072), UBA, WWE, and BH3 domains (1072–2394), C-terminal uncharacterized domain (2394–3617) alone, or HECT domain alone (Fig. 2B), and transfected them, respectively, into 293T cells together with a plasmid expressing V5-tagged HIV-1 IN CCD. Co-immunoprecipitation using an anti-FLAG antibody showed that the HIV-1 IN CCD associated with all of the truncation mutants of Huwe1 (Fig. 2C, lanes 2–4) except for the HECT domain mutant (Fig. 2C, lane 6). These results indicate that Huwe1 interacts with HIV-1 IN CCD through a broad region spanning 3500 amino acids.

3.3. Dispensable role of Huwe1 in early stage of HIV-1 infection

IN is a key component of the PIC [2]. Our preliminary experiment showed that PICs isolated from MoMLV-infected cells were immunoprecipitated by an anti-Huwe1 antibody, indicating the association of Huwe1 with the PIC (data not shown). Taken together with the result of physical interaction of IN and Huwe1, these data raise the possibility that Huwe1 may have a functional role during an early phase of virus replication. In order to assess the role of Huwe1 in HIV-1 infection, endogenous Huwe1 was depleted from a human T cell line, MT-4, by transduction of a lentivirus vector expressing miRNA against the Huwe1 ORF. Specific reduction of endogenous Huwe1 expression was confirmed by western blotting in the Huwe1 miRNA-expressing cells, but not in control miRNA-expressing cells (Fig. 3A). To estimate the efficiency of HIV-1 infection in the knockdown cells, a single-round replication assay was performed [7]. The Huwe1 knockdown and control MT-4 cells were used as target cells for infection by HIV-Luc pseudotyped with NL4-3 envelope (Env), and luciferase activity was measured 48 h after infection. As observed in Fig. 3B, a comparable level of luciferase activity was detected in Huwe1 knockdown and control cells. A similar result was also obtained by the infection with HIV-Luc pseudotyped with VSV-G (data not shown). In addition, when the cells were infected with replication competent HIV-1_{NL4-3}, no apparent difference in the amount of newly synthesized viral DNA was observed between Huwe1 knockdown and control cells (Fig. 3C). These results indicate that Huwe1 in target cells is not involved during the early steps of HIV-1 replication, from post-entry until viral gene expression.

3.4. Modulatory role of Huwe1 in HIV-1 infectivity

Some cellular interactors of HIV-1 IN have been shown to be involved in multiple steps of virus replication other than integration [14–16]. Thus, we next addressed the potential role of Huwe1 on the post-integrative steps in HIV-1 replication. Huwe1 knockdown and control cells were infected with HIV_{NL4-3} at a MOI of 0.001 for 2 h, and after washing, cells were cultured with fresh medium. When the culture supernatants were analyzed 3 days after infection, equivalent levels of $p24^{CA}$ were detected (Fig. 4A). In electron microscopy, the morphology of virus particles in Huwe1 knockdown cells was indistinguishable from the virus produced in control cells (Fig. 4B), indicating that virus particle production from Huwe1 knockdown and control cells were comparable. However, when the HIV-1 infectivity in the culture supernatants were compared by using TZM-bl indicator cells [30], we found that the infectivity of virus derived from Huwe1 knockdown cells was 2.2-fold higher than that of virus from control cells (Fig. 4C). This enhanced infectivity of HIV-1 was reproducibly observed with a separate preparation of Huwe1 knockdown cells (data not shown).

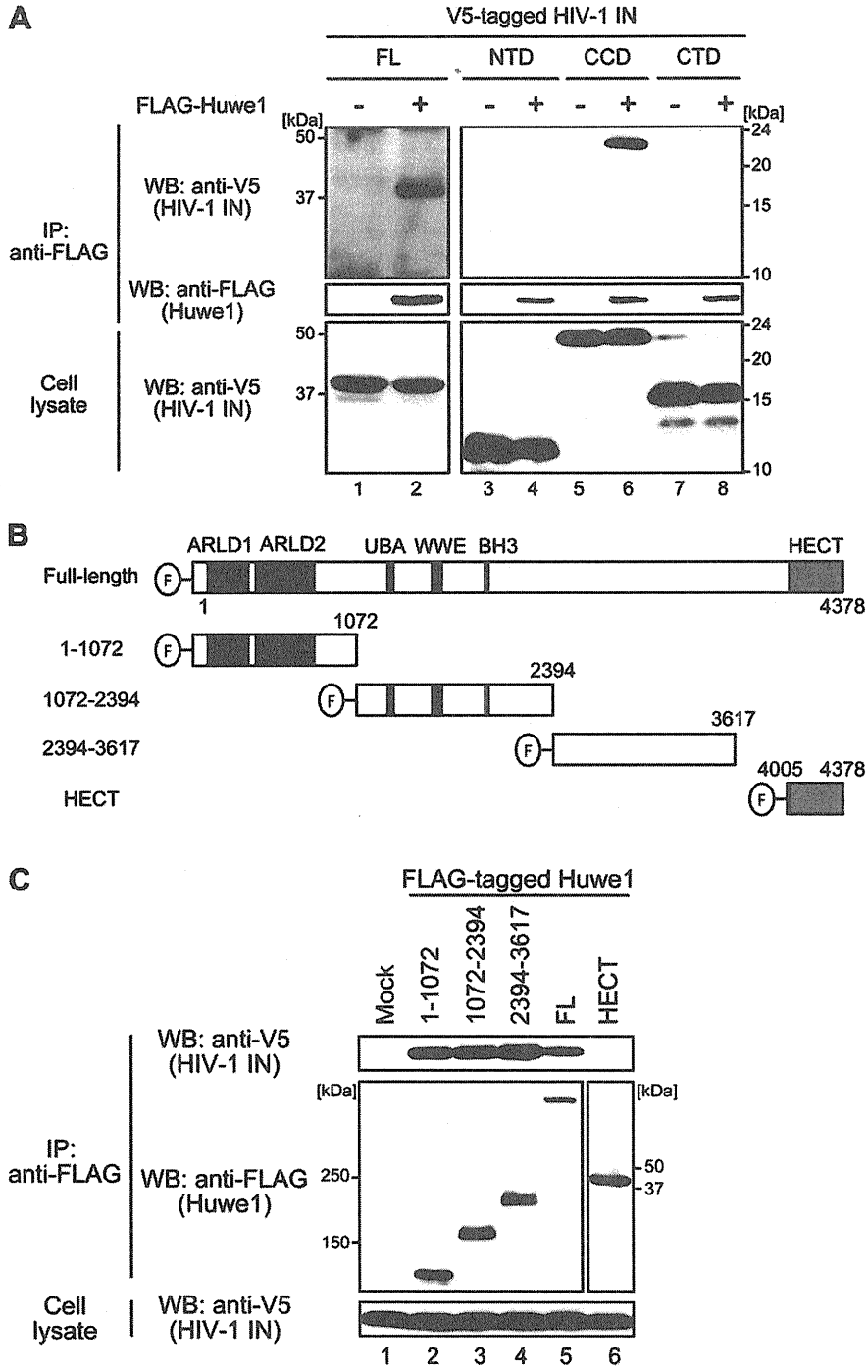

Fig. 2. Interaction domains between HIV-1 IN and Huwe1. (A) Binding domain in HIV-1 IN. FLAG-tagged Huwe1 was co-expressed with full-length (FL), N-terminus domain (NTD), catalytic core domain (CCD), or C-terminus domain (CTD) of V5-tagged HIV-1 IN in 293T cells. Cell lysates were subjected to immunoprecipitation (IP) using an anti-FLAG antibody, and HIV-1 IN and Huwe1 in immunoprecipitates were detected by western blotting analysis (WB) using anti-V5 and anti-FLAG antibodies, respectively. Masses of molecular weight standards are indicated at left (for FL IN) and right (for IN truncation mutants). (B) A schematic representation of Huwe1 used for co-immunoprecipitation assay with HIV-1 IN CCD. N-terminal FLAG (F)-tagged full-length Huwe1 and its truncation mutants (1–1072, 1072–2394, 2394–3617, and HECT) were constructed. ARLD, Armadillo repeat like domain. UBA, ubiquitin-associated domain. HECT, homologues to E6-AP carboxyl terminus domain. (C) Mapping of interaction domain in Huwe1. A series of FLAG-tagged Huwe1 (lane 5) or truncation mutants (lanes 2, 3, 4, and 6) were co-expressed with V5-tagged HIV-1 IN CCD in 293T cells and subjected to co-immunoprecipitation assay (IP) using an anti-FLAG antibody. Immunoprecipitates were analyzed by western blotting analysis (WB) using an anti-V5 (for HIV-1 IN CCD) or an anti-FLAG (for Huwe1) antibody. Masses of molecular weight standards are indicated at left (for Huwe1 1–1072, 1072–2394, 2394–3617, and FL) and right (for Huwe1 HECT).

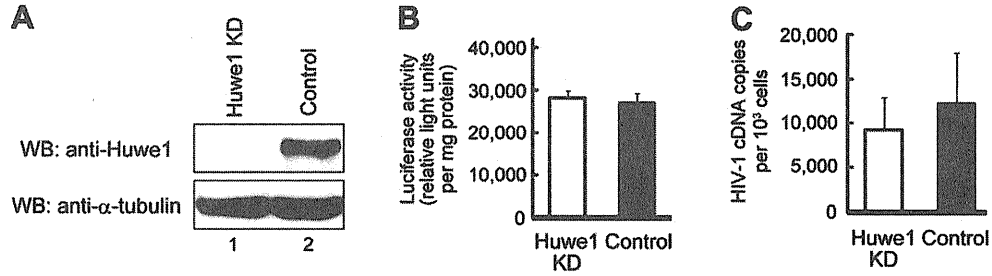

Fig. 3. Effect of Huwe1 depletion in the early stage of HIV-1 infection. (A) Establishment of Huwe1 knockdown (KD) cell. MT-4 cells were transduced with lentivirus vectors expressing miRNA against Huwe1 (lane 1) or control miRNA (lane 2). Expression of endogenous Huwe1 in both cell lines was examined by western blotting analysis (WB) using an anti-Huwe1 antibody. (B) Susceptibility of Huwe1 knockdown cells to single-round HIV-1 infection. Huwe1 knockdown (white bar) and control (black bar) MT-4 cells were infected with NL4-3 Env-pseudotyped HIV-Luc, and luciferase activity was measured 48 h after infection. (C) Level of HIV-1 DNA synthesis. Huwe1 knockdown and control MT-4 cells were infected with HIV-1_{NL4-3}, and the amount of newly synthesized viral DNA 24 h after infection was measured by quantitative PCR using HIV Tat-Rev specific primers. Data are expressed as mean value of three independent experiments with error bars indicating standard deviations.

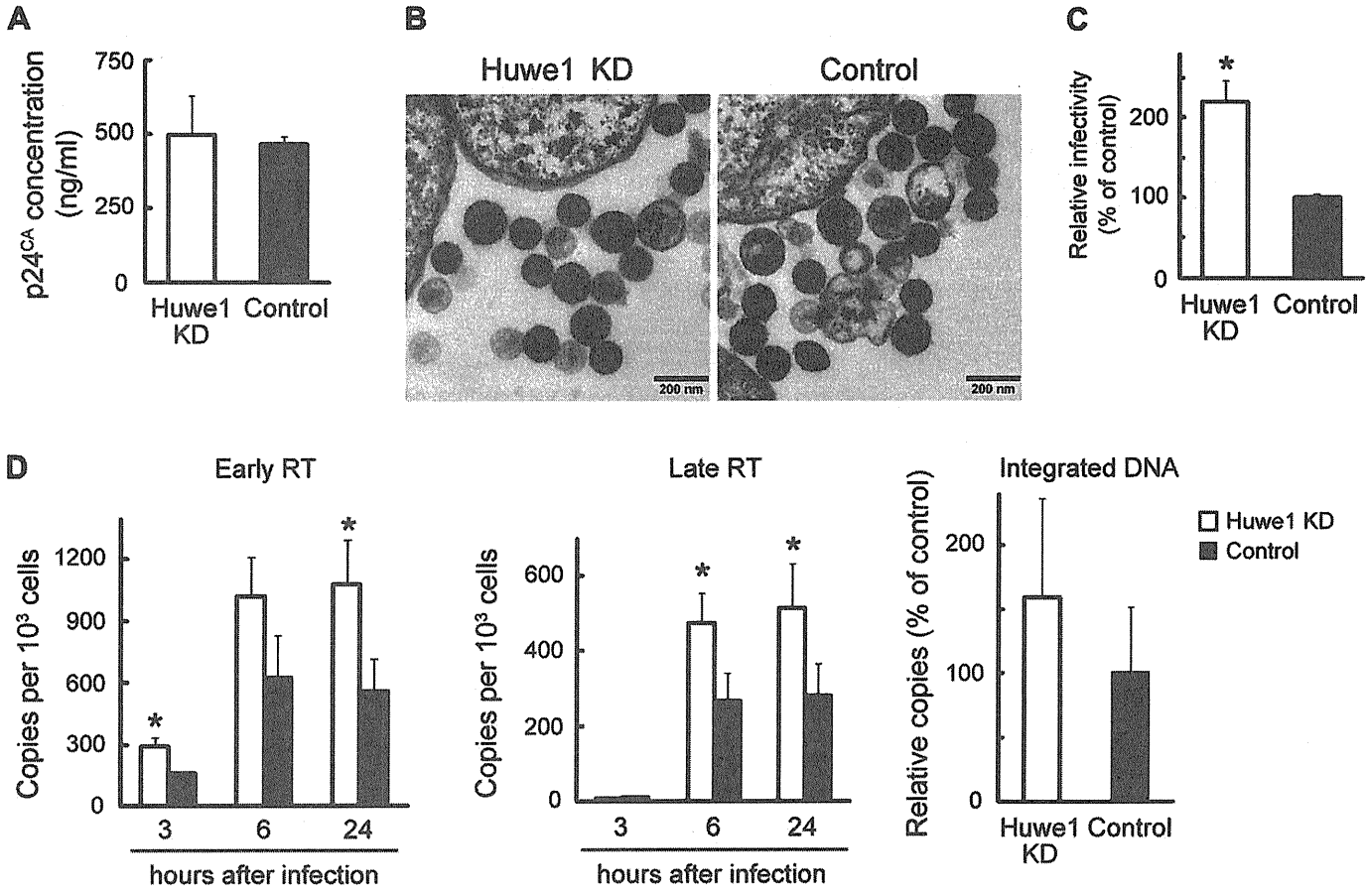

Fig. 4. Enhanced infectivity of HIV-1 produced from the Huwe1 knockdown cells. (A) Level of $p24^{CA}$ concentration in culture supernatants of HIV-1-infected cells. Huwe1 knockdown (KD, open bar) and control (closed bar) MT-4 cells were infected with HIV-1_{NL4-3} at a MOI of 0.001 for 2 h. The culture supernatants were collected 3 days after infection, and concentration of $p24^{CA}$ was measured by ELISA. (B) Electron microscopic analysis of HIV-1 particles. Virus-infected Huwe1 knockdown (left panel) and control (right panel) cells were analyzed by thin section electron microscopy. (C) Infectivity of HIV-1 derived from Huwe1 knockdown and control cells. Culture supernatants were collected 3 days after infection and added to TZM-bl indicator cells. Forty-eight hours after addition, β-galactosidase activity in the TZM-bl cells was measured. Results were normalized by $p24^{CA}$ concentration in the culture supernatants from producer cells. (D) Activity of reverse transcription and integration of HIV-1 derived from Huwe1 knockdown cells. Viruses produced in culture supernatants of Huwe1 knockdown (white bars) and control (black bars) cells were used for infection toward untransduced MT-4 cells. The levels of early and late RT products at point of 3, 6, and 24 h after infection and integrated DNA at point of 24 h after infection were analyzed by quantitative PCR. All data are expressed as mean value of three independent experiments with error bars indicating standard deviations. As for C and D, the P values versus control virus are <0.05 by Student's t test (*).

In order to clarify the steps in virus replication responsible for the enhanced infectivity, the culture supernatants from Huwe1 knockdown and control cells were added to parental (untransduced) MT-4 cells, and the efficiency of viral DNA synthesis and integration were measured by quantitative PCR. As shown in Fig. 4D, early and late RT products during the first day of infection were significantly increased in the MT-4 cells infected with Huwe1 knockdown cell-derived HIV-1 (left and middle panels). In parallel with the level of reverse transcription, increased amounts of integrated DNA was also detected in the cells infected with the Huwe1 knockdown cell-derived virus at 24 h after infection (Fig. 4D, right panel). Taken together, these data demonstrate that Huwe1 in virus producer cells has a negative impact on the formation of infectious HIV-1 particles, impeding the next round of infection.

3.5. Association of Huwe1 with the Gag-Pol through IN domain

During formation of HIV-1 particles, IN is expressed from provirus as a part of a 160 kDa Gag-Pol precursor [3]. Enhanced infectivity of HIV-1 produced from Huwe1-depleted cells (Fig. 4) raised the next possibility that Huwe1 associates with IN of Gag-Pol as well, thereby interfering with proper functions of the precursor protein during assembly of infectious virions. In order to test the interaction of Huwe1 with Gag-Pol polyprotein, we used an HIV-1 molecular clone expressing HA-tagged Gag-Pol without production of the Gag protein (Gag-Pol-HA, Fig. 5A). As expected, co-immunoprecipitation analysis revealed the interaction between HA-tagged Gag-Pol and FLAG-tagged Huwe1 in 293T cells (Fig. 5B, lane 2). When we used another molecular clone expressing HA-tagged Gag-Pol lacking the IN region (Gag-Pol-HA/ΔIN, Fig. 5A), FLAG-tagged Huwe1 did not co-immunoprecipitate with the mutant Gag-Pol (Fig. 5B, lane 4). This data indicates that Huwe1 binds to HIV-1 Gag-Pol protein and the interaction is in an IN region dependent manner.

4. Discussion

Genetic studies of HIV-1 DNA have demonstrated that certain mutations of the *IN* gene are pleiotropic, and the effects are often observed at stages distinct from integration [5–11]. Similarly, a number of cellular interactors of IN have been reported, with some of the factors appearing to have functional roles in reverse transcription, gene expression, and infectious particle production [12]. For instance, INI1, the first IN-binding protein identified, is reported to have an effect on infectious particle production in the HIV-1 replication cycle through incorporation into virions [16,19]. These evidence indicate that protein–protein interactions between IN and cellular factor(s) would influence multiple steps of retrovirus replication. In this study, we report that Huwe1, a new cellular partner for IN and Gag-Pol, somehow modulates efficient formation of infectious virions on the post-integrative steps in

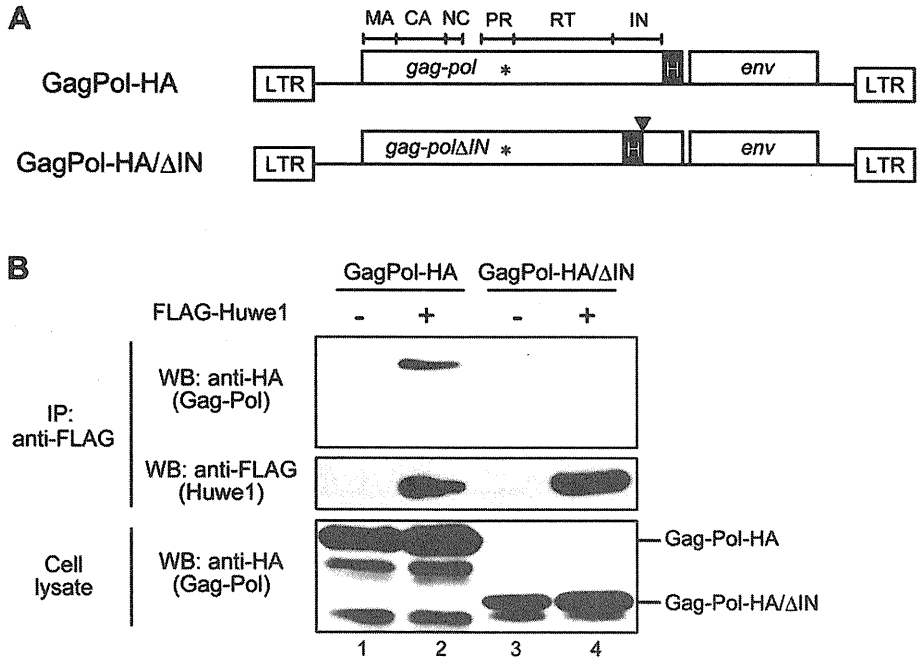

Fig. 5. Interaction of Huwe1 with HIV-1 Gag-Pol protein through IN domain. (A) A schematic representation of HIV-1 molecular clones expressing HA-tagged Gag-Pol polyproteins. HA (H) tag sequence was inserted in the C-terminus of the *pol* gene (Gag-Pol-HA). For the expression of HA-tagged Gag-Pol lacking IN region (Gag-Pol-HA/ΔIN), HA tag sequence (H) and subsequent premature termination codon (arrowhead) were introduced at the junction between RT and IN regions. All constructs were generated from pNL4-3 bearing an inactive PR, in which Asp-25 had been replaced with Ala (asterisks) [32]. (B) Interaction of Huwe1 with Gag-Pol through the IN region. FLAG-tagged Huwe1 were co-expressed with either Gag-Pol-HA or Gag-Pol-HA/ΔIN in 293T cells and subjected to immunoprecipitation assay (IP) using an anti-FLAG antibody. Gag-Pol and Huwe1 in immunoprecipitates were detected by western blotting analysis (WB) using anti-HA and anti-FLAG antibodies, respectively.

HIV-1 replication. Our results provide an intriguing insight into the role of an IN-binding protein in the production of HIV-1 virions.

So far, identification of IN-binding proteins have been conducted mostly by yeast two-hybrid screenings or co-immunoprecipitation assays [2]. In the present study, by employing a TAP procedure, tubulins and Huwe1 were identified as cellular interactors of MoMLV and HIV-1 IN (Fig. 1). α- and β-tubulins are the building blocks of microtubules and known to form heterodimers [36]. Microtubule is a key component of the cytoskeleton that regulates development and maintenance of cell shape, transport of components throughout cells, cell signaling, cell division, and mitosis [36]. The microtubule cytoskeletal network is also shown to be implicated in intracellular movement of retroviruses, and indeed several viral proteins are reported to interact with microtubule and its related factors [37]. Consistent with our data, previous studies have also reported that HIV-1 IN interacts with yeast microtubule-associated protein and human β-tubulin [2,38]. Although the physiological role of the binding of IN to microtubules is unclear, this interaction may function as one of the driving forces for intracellular trafficking of incoming viral core complexes such as PICs.

Huwe1 is a 482 kDa HECT-type E3 ubiquitin ligase and is also named Mule, ARF-BP-1, HectH9, $E3^{Histone}$, LASU1, and UREB1 [33]. This large protein was first identified as an E3 ligase that catalyzes ubiquitination of p53 and c-Myc [34,35]. Later on, histones, Cdc6, and N-myc were reported as substrates for Huwe1 [33]. Ubiquitination of these proteins by Huwe1 are implicated in proliferation, differentiation, apoptosis, gene expression, and DNA damage responses in cells [33]. However, there have been no reports regarding the interaction between Huwe1 and retroviral proteins.

In addition to the physical interaction with IN, we revealed that Huwe1 specifically binds to HIV-1 Gag-Pol protein in a C-terminal IN region dependent manner (Fig. 5). Furthermore, depletion of endogenous Huwe1 in T cells resulted in increasing infectivity of HIV-1 virions released from these cells (Fig. 4), suggesting that Huwe1 may regulate formation/production of virus particles in producer cells via an association with IN in the context of Gag-Pol. If this is the case, then how does Huwe1 modulate the HIV-1 infectivity? A number of studies have demonstrated that, during HIV-1 particle assembly, Gag and Env proteins are associated with lipid raft membrane subdomains, which is characterized by their insolubility against nonionic detergents such as NP-40 and Triton X-100 [39]. Likewise, it has been shown that Gag-Pol protein is also taken up by the detergent-resistant membrane (DRM) fraction through multimerization with Gag protein [40]. Since we could not find the incorporation of Huwe1 into HIV-1 virions (data not shown), one possibility would be that Huwe1 blocks the proper intracellular localization of the Gag-Pol precursor in virus producer cells: Huwe1 present in certain compartments of the cytoplasm could sequester a Gag-Pol precursor through its interaction with the IN region and, consequently, interfere with proper localization of Gag-Pol to specialized areas of the plasma membrane such as lipid rafts, where assembly of infectious virus particles take place with Gag. Supporting this hypothesis, our preliminary experiment showed that Huwe1 is indeed distributed in a NP-40-soluble fraction, whereas caveolin, a structural membrane protein of caveolae enriched in lipid rafts [41], remained in an insoluble fraction (data not shown). Therefore, Gag-Pol protein may accumulate in the DRM more efficiently by Huwe1 depletion, resulting in a significant increase in the virus infectivity (Fig. 4). Further biochemical analysis will be required to determine whether the distribution of Huwe1 disrupts proper association of Gag-Pol with lipid raft domains that serve as platforms for virion assembly.

An alternative and likely explanation for the negative modulation of HIV-1 infectivity by Huwe1 is that Huwe1 would mask the IN region of Gag-Pol precursor, thereby impeding the incorporation of another cellular factor(s) into virions, which is necessary for the next round of infection. Recent evidence indicates that INI1, a core subunit of the chromatin-remodeling complex SWI/SNF, is specifically packaged into HIV-1 virions [42]. It has been also shown that ectopic expression of a fragment of INI1 has a dominant negative effect on HIV-1 virion production via its interaction with IN within the context of Gag-Pol [16]. Another study revealed that IN and INI1 selectively recruits other cellular factors SAP18 and HDAC1, the components of a Sin3a-HDAC1 complex, into HIV-1 virions [43]. Interestingly, virion-associated HDAC1 activity appeared to enhance virus infectivity without any affect on particle production, and the enhancement of infectivity occurred at the early reverse transcription step in the next target cells [43]. In parallel with this observation, our results show that HIV-1 derived from Huwe1 knockdown cells exhibited increased activity in the synthesis of early RT products, albeit virion production was not affected (Fig. 4). Presently, our attempts to determine whether the recruitment of IN interacting proteins is competed with by the presence of Huwe1 will clarify the molecular mechanism underlying Huwe1-mediated modulation of HIV-1 infectivity.

As mentioned above, Huwe1 is a HECT-type E3 ubiquitin ligase that targets cellular transcription factors, histones, and anti-apoptotic proteins for ubiquitination [33]. One question to ponder would be, does the ubiquitin ligase activity link to the modulatory function of Huwe1 in HIV-1 replication? HIV-1 IN is well known to undergo proteasome-mediated degradation via ubiquitination [15]. When we performed an *in vivo* ubiquitination assay in which Myc-tagged ubiquitin (Myc-Ub) was co-expressed with HIV-1 IN in 293T cells, and subsequently Myc-Ub-conjugated IN was isolated by immunoprecipitation, a comparable level of polyubiquitylated IN was detected from Huwe1 knockdown and control cells (data not shown). In addition, although we found that HIV-1 Gag-Pol is also polyubiquitylated in a similar *in vivo* ubiquitination assay [44], Huwe1 knockdown did not have an influence on the Gag-Pol ubiquitination (data not shown). Consistent with these results, neither the knockdown nor the overexpression of Huwe1 affected the stability of HIV-1 IN and Gag-Pol in 293T cells (data not shown), indicating that Huwe1 is not involved in ubiquitination and subsequent proteasomal-degradation of IN and Gag-Pol proteins. Given the result that Huwe1 associated with IN

through an extensive region independently of the C-terminal HECT domain, the catalytic domain responsible for the transfer of ubiquitin to substrate (Fig. 2C), one could speculate that Huwe1 acts as a scaffolding modulator, which interferes with proper localization and/or function of Gag-Pol precursor in HIV-1 producer cells.

In summary, the present study identified Huwe1 as a novel interactor of HIV-1 IN and Gag-Pol that has a negative impact on the formation of infectious virus. It should be noted that, by a recent report using a large-scale siRNA screening, Huwe1 has been found as a host factor implicated in HIV-1 infectivity [45]. However, in contrast to our study, knocking down of Huwe1 by siRNA in HeLa cells diminished virus infectivity to 37% compared to the virus derived from control cells [45]. Although we could not observe any effect of Huwe1 knock-down in HeLa cells on the virus infectivity, it will be intriguing to analyze cellular differences in the role of Huwe1 in HIV-1 replication. Additionally, further analysis of the mechanism by which Huwe1 modulates virus infectivity could be the basis of a future strategy for the treatment of HIV-1 infection.

Acknowledgements

We thank Giulio Superti-Furga (Research Center for Molecular Medicine) for providing the pCeMM-NTAP(GS) vector, Yoshihiko Fujioka (Osaka Medical College) for assistance with the EM, and Kazuhiro Iwai (Osaka University) and Akifumi Takaori-Kondo (Kyoto University) for support in the *in vivo* ubiquitination assay. We are also grateful to Peter Gee for proofreading and comments on the manuscript and to members of the Laboratory of Viral Pathogenesis and Laboratory for Host Factors for support of experimental techniques and helpful discussions. This work was supported by grants from the Ministry of Health, Labor and Welfare and the Ministry of Education, Culture, Sports, Science and Technology of Japan. SPY was supported by Research Fellowships of the Japan Society for the Promotion of Science for Young Scientists.

References

[1] M.K. Lewinski, F.D. Bushman, Retroviral DNA integration–mechanism and consequences, Adv. Genet. 55 (2005) 147–181.
[2] F. Turlure, E. Devroe, P.A. Silver, A. Engelman, Human cell proteins and human immunodeficiency virus DNA integration, Front. Biosci. 9 (2004) 3187–3208.
[3] R. Swanstrom, J.W. Wills, Synthesis, Assembly, and Processing of Viral Proteins. Cold Spring Harbor Laboratory, Cold Spring Harbor, N.Y., 1997.
[4] X. Wu, H. Liu, H. Xiao, J.A. Conway, E. Hunter, J.C. Kappes, Functional RT and IN incorporated into HIV-1 particles independently of the Gag/Pol precursor protein, EMBO J. 16 (1997) 5113–5122.
[5] C.G. Shin, B. Taddeo, W.A. Haseltine, C.M. Farnet, Genetic analysis of the human immunodeficiency virus type 1 integrase protein, J. Virol. 68 (1994) 1633–1642.
[6] A. Engelman, G. Englund, J.M. Orenstein, M.A. Martin, R. Craigie, Multiple effects of mutations in human immunodeficiency virus type 1 integrase on viral replication, J. Virol. 69 (1995) 2729–2736.
[7] T. Masuda, V. Planelles, P. Krogstad, I.S. Chen, Genetic analysis of human immunodeficiency virus type 1 integrase and the U3 att site: unusual phenotype of mutants in the zinc finger-like domain, J. Virol. 69 (1995) 6687–6696.
[8] A.D. Leavitt, G. Robles, N. Alesandro, H.E. Varmus, Human immunodeficiency virus type 1 integrase mutants retain in vitro integrase activity yet fail to integrate viral DNA efficiently during infection, J. Virol. 70 (1996) 721–728.
[9] A. Bukovsky, H. Gottlinger, Lack of integrase can markedly affect human immunodeficiency virus type 1 particle production in the presence of an active viral protease, J. Virol. 70 (1996) 6820–6825.
[10] N. Tsurutani, M. Kubo, Y. Maeda, T. Ohashi, N. Yamamoto, M. Kannagi, T. Masuda, Identification of critical amino acid residues in human immunodeficiency virus type 1 IN required for efficient proviral DNA formation at steps prior to integration in dividing and nondividing cells, J. Virol. 74 (2000) 4795–4806.
[11] M.S. Briones, C.W. Dobard, S.A. Chow, Role of human immunodeficiency virus type 1 integrase in uncoating of the viral core, J. Virol. 84 (2010) 5181–5190.
[12] L.Q. Al-Mawsawi, N. Neamati, Blocking interactions between HIV-1 integrase and cellular cofactors: an emerging anti-retroviral strategy, Trends Pharmacol. Sci. 28 (2007) 526–535.
[13] B. Studamire, S.P. Goff, Host proteins interacting with the Moloney murine leukemia virus integrase: multiple transcriptional regulators and chromatin binding factors, Retrovirology 5 (2008) 48.
[14] S. Hamamoto, H. Nishitsuji, T. Amagasa, M. Kannagi, T. Masuda, Identification of a novel human immunodeficiency virus type 1 integrase interactor, Gemin2, that facilitates efficient viral cDNA synthesis in vivo, J. Virol. 80 (2006) 5670–5677.
[15] A. Mousnier, N. Kubat, A. Massias-Simon, E. Segeral, J.C. Rain, R. Benarous, S. Emiliani, C. Dargemont, von Hippel Lindau binding protein 1-mediated degradation of integrase affects HIV-1 gene expression at a postintegration step, Proc. Natl. Acad. Sci. U.S.A 104 (2007) 13615–13620.
[16] E. Yung, M. Sorin, A. Pal, E. Craig, A. Morozov, O. Delattre, J. Kappes, D. Ott, G.V. Kalpana, Inhibition of HIV-1 virion production by a transdominant mutant of integrase interactor 1, Nat. Med. 7 (2001) 920–926.
[17] F. Christ, W. Thys, J. De Rijck, R. Gijsbers, A. Albanese, D. Arosio, S. Emiliani, J.C. Rain, R. Benarous, A. Cereseto, Z. Debyser, Transportin-SR2 imports HIV into the nucleus, Curr. Biol. 18 (2008) 1192–1202.
[18] C.L. Woodward, S. Prakobwanakit, S. Mosessian, S.A. Chow, Integrase interacts with nucleoporin NUP153 to mediate the nuclear import of human immunodeficiency virus type 1, J. Virol. 83 (2009) 6522–6533.
[19] M. Sorin, E. Yung, X. Wu, G.V. Kalpana, HIV-1 replication in cell lines harboring INI1/hSNF5 mutations, Retrovirology 3 (2006) 56.
[20] X. Wei, J.M. Decker, H. Liu, Z. Zhang, R.B. Arani, J.M. Kilby, M.S. Saag, X. Wu, G.M. Shaw, J.C. Kappes, Emergence of resistant human immunodeficiency virus type 1 in patients receiving fusion inhibitor (T-20) monotherapy, Antimicrob. Agents Chemother. 46 (2002) 1896–1905.
[21] J. Colicelli, S.P. Goff, Sequence and spacing requirements of a retrovirus integration site, J. Mol. Biol. 199 (1988) 47–59.
[22] T. Burckstummer, K.L. Bennett, A. Preradovic, G. Schutze, O. Hantschel, G. Superti-Furga, A. Bauch, An efficient tandem affinity purification procedure for interaction proteomics in mammalian cells, Nat. Methods 3 (2006) 1013–1019.
[23] H. Nishitsuji, T. Hayashi, T. Takahashi, M. Miyano, M. Kannagi, T. Masuda, Augmentation of reverse transcription by integrase through an interaction with host factor, SIP1/Gemin2 Is critical for HIV-1 infection, PLoS One 4 (2009) e7825.
[24] O.N. Jensen, A. Podtelejnikov, M. Mann, Delayed extraction improves specificity in database searches by matrix-assisted laser desorption/ionization peptide maps, Rapid Commun. Mass Spectrom. 10 (1996) 1371–1378.
[25] Y. Shinoda, K. Hieda, Y. Koyanagi, Y. Suzuki, Efficient transduction of cytotoxic and anti-HIV-1 genes by a gene-regulatable lentiviral vector, Virus Genes 39 (2009) 165–175.
[26] K. Niwano, M. Arai, N. Koitabashi, A. Watanabe, Y. Ikeda, H. Miyoshi, M. Kurabayashi, Lentiviral vector-mediated SERCA2 gene transfer protects against heart failure and left ventricular remodeling after myocardial infarction in rats, Mol. Ther. 16 (2008) 1026–1032.
[27] K. Sato, J. Aoki, N. Misawa, E. Daikoku, K. Sano, Y. Tanaka, Y. Koyanagi, Modulation of human immunodeficiency virus type 1 infectivity through incorporation of tetraspanin proteins, J. Virol. 82 (2008) 1021–1033.

[28] Y. Kawano, Y. Tanaka, N. Misawa, R. Tanaka, J.I. Kira, T. Kimura, M. Fukushi, K. Sano, T. Goto, M. Nakai, T. Kobayashi, N. Yamamoto, Y. Koyanagi, Mutational analysis of human immunodeficiency virus type 1 (HIV-1) accessory genes: requirement of a site in the nef gene for HIV-1 replication in activated $CD4^+$ T cells in vitro and in vivo, J. Virol. 71 (1997) 8456–8466.

[29] J.A. Zack, S.J. Arrigo, S.R. Weitsman, A.S. Go, A. Haislip, I.S. Chen, HIV-1 entry into quiescent primary lymphocytes: molecular analysis reveals a labile, latent viral structure, Cell 61 (1990) 213–222.

[30] S.J. Neil, T. Zang, P.D. Bieniasz, Tetherin inhibits retrovirus release and is antagonized by HIV-1 Vpu, Nature 451 (2008) 425–430.

[31] Y. Suzuki, N. Misawa, C. Sato, H. Ebina, T. Masuda, N. Yamamoto, Y. Koyanagi, Quantitative analysis of human immunodeficiency virus type 1 DNA dynamics by real-time PCR: integration efficiency in stimulated and unstimulated peripheral blood mononuclear cells, Virus Genes 27 (2003) 177–188.

[32] M. Huang, J.M. Orenstein, M.A. Martin, E.O. Freed, $p6^{Gag}$ is required for particle production from full-length human immunodeficiency virus type 1 molecular clones expressing protease, J. Virol. 69 (1995) 6810–6818.

[33] F. Bernassola, M. Karin, A. Ciechanover, G. Melino, The HECT family of E3 ubiquitin ligases: multiple players in cancer development, Cancer Cell 14 (2008) 10–21.

[34] D. Chen, N. Kon, M. Li, W. Zhang, J. Qin, W. Gu, ARF-BP1/Mule is a critical mediator of the ARF tumor suppressor, Cell 121 (2005) 1071–1083.

[35] Q. Zhong, W. Gao, F. Du, X. Wang, Mule/ARF-BP1, a BH3-only E3 ubiquitin ligase, catalyzes the polyubiquitination of Mcl-1 and regulates apoptosis, Cell 121 (2005) 1085–1095.

[36] R.H. Wade, A.A. Hyman, Microtubule structure and dynamics, Curr. Opin. Cell Biol. 9 (1997) 12–17.

[37] M.H. Naghavi, S.P. Goff, Retroviral proteins that interact with the host cell cytoskeleton, Curr. Opin. Immunol. 19 (2007) 402–407.

[38] V.R. de Soultrait, A. Caumont, P. Durrens, C. Calmels, V. Parissi, P. Recordon, E. Bon, C. Desjobert, L. Tarrago-Litvak, M. Fournier, HIV-1 integrase interacts with yeast microtubule-associated proteins, Biochim. Biophys. Acta 1575 (2002) 40–48.

[39] A. Ono, Relationships between plasma membrane microdomains and HIV-1 assembly, Biol. Cell 102 (2010) 335–350.

[40] R. Halwani, A. Khorchid, S. Cen, L. Kleiman, Rapid localization of Gag/GagPol complexes to detergent-resistant membrane during the assembly of human immunodeficiency virus type 1, J. Virol. 77 (2003) 3973–3984.

[41] K. Simons, D. Toomre, Lipid rafts and signal transduction, Nat. Rev. Mol. Cell Biol. 1 (2000) 31–39.

[42] E. Yung, M. Sorin, E.J. Wang, S. Perumal, D. Ott, G.V. Kalpana, Specificity of interaction of INI1/hSNF5 with retroviral integrases and its functional significance, J. Virol. 78 (2004) 2222–2231.

[43] M. Sorin, J. Cano, S. Das, S. Mathew, X. Wu, K.P. Davies, X. Shi, S.W. Cheng, D. Ott, G.V. Kalpana, Recruitment of a SAP18-HDAC1 complex into HIV-1 virions and its requirement for viral replication, PLoS Pathog. 5 (2009) e1000463.

[44] T. Izumi, A. Takaori-Kondo, K. Shirakawa, H. Higashitsuji, K. Itoh, K. Io, M. Matsui, K. Iwai, H. Kondoh, T. Sato, M. Tomonaga, S. Ikeda, H. Akari, Y. Koyanagi, J. Fujita, T. Uchiyama, MDM2 is a novel E3 ligase for HIV-1 Vif, Retrovirology 6 (2009) 1.

[45] A.L. Brass, D.M. Dykxhoorn, Y. Benita, N. Yan, A. Engelman, R.J. Xavier, J. Lieberman, S.J. Elledge, Identification of host proteins required for HIV infection through a functional genomic screen, Science 319 (2008) 921–926.

OPEN ACCESS Freely available online

PLoS one

Cloning and Characterization of the Antiviral Activity of Feline Tetherin/BST-2

Aiko Fukuma[1,2,3], Masumi Abe[2], Yuko Morikawa[3], Takayuki Miyazawa[4], Jiro Yasuda[1,2]*

1 Department of Emerging Infectious Diseases, Institute of Tropical Medicine, Nagasaki University, Nagasaki, Japan, 2 Fifth Biology Section for Microbiology, First Department of Forensic Science, National Research Institute of Police Science, Kashiwa, Japan, 3 Kitasato Institute for Life Sciences and Graduate School for Infection Control, Kitasato University, Tokyo, Japan, 4 Laboratory of Signal Transduction, Institute for Virus Research, Kyoto University, Kyoto, Japan

Abstract

Human Tetherin/BST-2 has recently been identified as a cellular antiviral factor that blocks the release of various enveloped viruses. In this study, we cloned a cDNA fragment encoding a feline homolog of Tetherin/BST-2 and characterized the protein product. The degree of amino acid sequence identity between human Tetherin/BST-2 and the feline homolog was 44.4%. Similar to human Tetherin/BST-2, the expression of feline Tetherin/BST-2 mRNA was inducible by type I interferon (IFN). Exogenous expression of feline Tetherin/BST-2 efficiently inhibited the release of feline endogenous retrovirus RD-114. The extracellular domain of feline Tetherin/BST-2 has two putative *N*-linked glycosylation sites, N79 and N119. Complete loss of *N*-linked glycosylation by introduction of mutations into both sites resulted in almost complete abolition of its antiviral activity. In addition, feline Tetherin/BST-2 was insensitive to antagonism by HIV-1 Vpu, although the antiviral activity of human Tetherin/BST-2 was antagonized by HIV-1 Vpu. Our data suggest that feline Tetherin/BST-2 functions as a part of IFN-induced innate immunity against virus infection and that the induction of feline Tetherin/BST-2 *in vivo* may be effective as a novel antiviral strategy for viral infection.

Citation: Fukuma A, Abe M, Morikawa Y, Miyazawa T, Yasuda J (2011) Cloning and Characterization of the Antiviral Activity of Feline Tetherin/BST-2. PLoS ONE 6(3): e18247. doi:10.1371/journal.pone.0018247

Editor: David Harrich, Queensland Institute of Medical Research, Australia

Received October 28, 2010; **Accepted** March 1, 2011; **Published** March 29, 2011

Funding: This work was supported by grants from the Bio-Oriented Technology Research Advancement Institution and the Japan Society for the Promotion of Science. The funders had no role in study design, data collection and analysis, decision to publish, or preparation of the manuscript.

Competing Interests: The authors have declared that no competing interests exist.

* E-mail: j-yasuda@nagasaki-u.ac.jp

Introduction

Human Tetherin/BST-2 (also referred to as CD317 or HM1.24) was first identified as a cellular restriction factor that blocks the release of HIV-1 in the absence of the viral accessory protein, Vpu [1]. Subsequent studies have shown that human Tetherin/BST-2 also inhibits the release of other retroviruses, filoviruses, arenaviruses, and herpesviruses [1–7].

Tetherin/BST-2 is a type II integral membrane protein consisting of an N-terminal cytoplasmic tail, a transmembrane domain, followed by an extracellular domain important for dimerization, and a glycophosphatidyl inositol (GPI) lipid anchor at its C-terminus [8]. The extracellular domain of Tetherin/BST-2 has two putative *N*-linked glycosylation sites, which are highly conserved at the same positions among human, rhesus monkey, dog, pig, rat, and mouse, and orthologs have been identified that are actually glycosylated heterogeneously [8,9]. Previously, we showed that *N*-linked glycosylation is dispensable for the antiviral activity of human Tetherin/BST-2 against Lassa and Marburg viruses [6]. On the other hand, there are conflicting data regarding the role of *N*-linked glycosylation on the antiviral activity of human Tetherin/BST-2 against HIV-1. Andrew *et al.* reported that *N*-linked glycosylation is not important for inhibition of HIV-1 virus release, while Perez-Caballero *et al.* showed that *N*-linked glycosylation, especially at the second site, is important for the antiviral activity of human Tetherin/BST-2 against HIV-1 [10,11].

Human Tetherin/BST-2 is constitutively expressed in terminally differentiated B cells, bone marrow stromal cells, and plasmacytoid dendritic cells, and is upregulated in various cell types on treatment with type I and type II interferon (IFN) [12,13]. Therefore, Tetherin/BST-2 is thought to be involved in antiviral host defense as an innate immunity mechanism. It has also been reported that several viruses encode antagonists, such as HIV-1 Vpu, HIV-2 Env, SIVmac/cpz/gor Nef, Ebola virus GP, and Kaposi's sarcoma-associated herpesvirus (KSHV) K5, which antagonize the antiviral activity of Tetherin/BST-2 [1,5,7,14–17].

The cat genome contains an infectious endogenous retrovirus (ERV) named RD-114 [18]. Several feline cell lines including Crandell-Rees feline kidney (CRFK) cells constitutively express infectious RD-114 [19,20]. Therefore, there is concern regarding contamination by RD-114 in vaccines, as these cells have been used to grow several live attenuated vaccines for pets and cattle. In fact, we recently reported the isolation of an infectious RD-114 in a proportion of live attenuated vaccines for pets [21]. RD-114 is considered to be a polytropic virus, since it efficiently infects feline cells as well as human and dog cells [19,22]. Although the pathogenicity of RD-114 has not been determined, it has potential risks in that interspecies transmission may induce unpredictable diseases. However, it is very difficult to completely exclude the proviral DNA of RD-114 from cells, as ERVs are usually integrated into multiple loci in the host chromosomes [18].

In this study, to investigate the potential of Tetherin/BST-2 to regulate the production of RD-114 from cells, we cloned and characterized the feline homolog of Tetherin/BST-2 and examined its ability to restrict the release of RD-114 from cells.

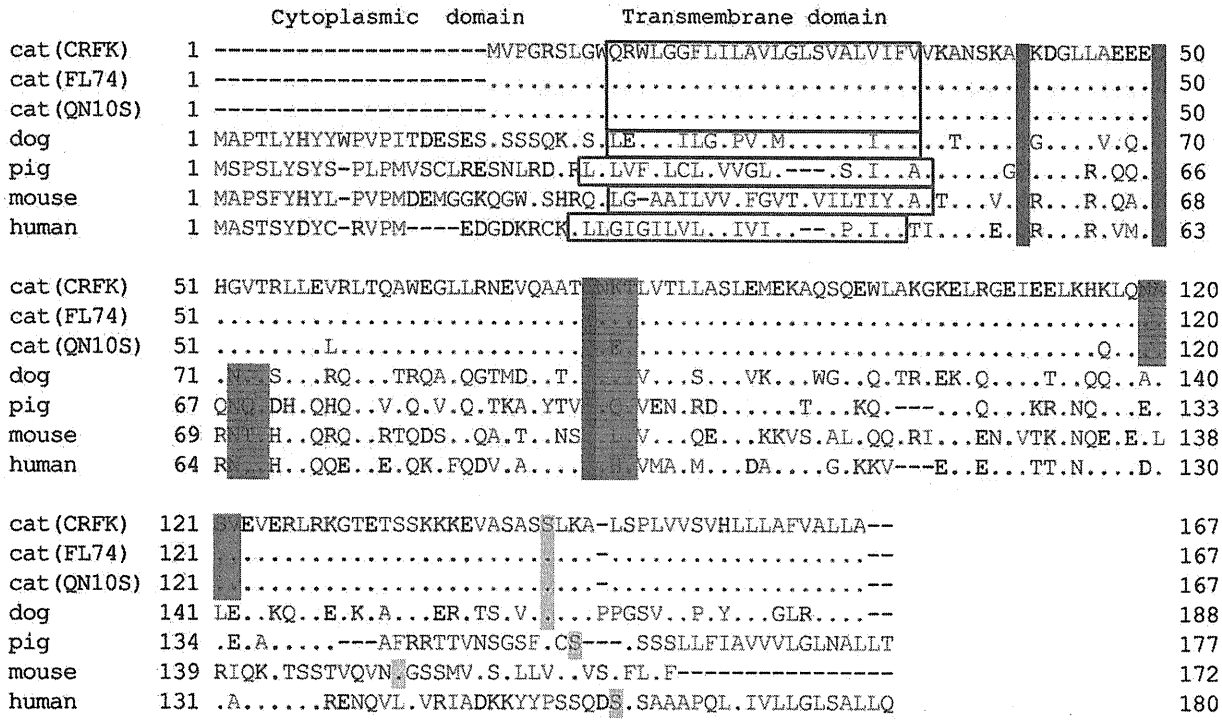

Figure 1. Comparison of the predicted amino acid sequences of cat, dog, pig, mouse, and human Tetherin/BST-2 homologs. Cat (CRFK, FL74, and QN10S cells), dog, pig, mouse, and human Tetherin/BST-2 sequences were analyzed and aligned using GENETYX ver. 8 (GENETYX, Tokyo, Japan). The predicted transmembrane domain is boxed. Three Cys residues in the extracellular domain, which are important for dimerization, are shown with a red background. Two putative glycosylation sites are shown with a blue background. Ser residues of the predicted cleavage site prior to addition of a GPI anchor are shown with a yellow background.
doi:10.1371/journal.pone.0018247.g001

Materials and Methods

Cells

Human embryonic kidney (HEK) 293T cells, Crandell-Rees feline kidney (CRFK) cells, and QN10S cells were maintained at 37°C in a 5% CO_2 incubator in Dulbecco's modified Eagle's medium (Sigma, St. Louis, MO) supplemented with 10% fetal bovine serum and penicillin/streptomycin. FL74 cells (feline T-lymphoblastoid cell line) were maintained at 37°C in a 5% CO_2 incubator in RPMI 1640 medium (Sigma) supplemented with 10% fetal bovine serum and penicillin/streptomycin.

Cloning of the feline Tetherin/BST-2 gene

The primer TethConF (5′-TCACCATCAAGGCCAACAGC-3′), corresponding to a sequence conserved among Tetherin/BST-2 genes from various species reported to date, was designed to clone feline Tetherin/BST-2. RT-PCR was performed using a PrimeSTAR RT-PCR Kit (Takara, Shiga, Japan), with total RNA extracted from IFN-treated CRFK cells as the template, according to the manufacturer's protocols. Partial cDNA fragments of feline Tetherin/BST-2 with high degrees of identity to human Tetherin/BST-2 were amplified. To determine the initiation site of the coding sequence (CDS) of feline Tetherin/BST-2, 5′-RACE was performed with a Takara 5′-Full RACE Core Set according to the manufacturer's protocols (Takara), using total RNA extracted from IFN-treated CRFK, FL74, or QN10S cells as the template. The feline Tetherin/BST-2 gene was identified. The intact CDS of feline Tetherin/BST-2 was amplified again by RT-PCR, and then cloned into pCDNFL, which was constructed from pcDNA3.1 (Invitrogen, Carlsbad, CA) to express a protein containing a FLAG-tag at the N-terminus [6,23]. The expression plasmid for feline Tetherin/BST-2 was named pfelTeth-FL.

Plasmids

The plasmids carrying human Tetherin/BST-2 or HIV-1 Vpu, pTeth-FL or pVpu-Myc, respectively, and the plasmid containing an intact infectious clone of RD-114, pTERD-114, were described previously [6,24]. The glycosylation mutants of feline Tetherin/BST-2 with asparagine to alanine substitution(s) at position 79 and/or 119, N79A, N119A, and N79A/N119A, were generated from pfelTeth-FL using a QuikChange II site-directed mutagenesis kit (Stratagene, La Jolla, CA).

Quantification of feline Tetherin/BST-2 mRNA by real-time RT-PCR

To examine the induction of feline Tetherin/BST-2 by IFN, CRFK cells were treated for 24 h in the presence of 100 or 1,000 units/ml IFN-αA/D (Sigma) and then total cellular RNA was extracted from pelleted cells using an RNeasy Mini kit (Qiagen, Valencia, CA). Real-time RT-PCR was performed using the feline Tetherin/BST-2 primers, 5′-GGAGTGTCACGGTGTCACCC-3′ (forward) and 5′-CCTCAATCTCTCCCCGAAGCTC-3′ (reverse), and the 18S rRNA primers, 5′-GACGACCCATTC-GAACGTCT-3′ (forward) and 5′-TGCTGCCTTCCTTG-GATGTG-3′ (reverse). Amplification was performed with a One-Step SYBR RT-PCR Kit (Takara) according to the manufacturer's protocols using a Smart Cycler II System (Cepheid, Sunnyvale, CA).

Assay for antiviral activity of Tetherin/BST-2 against RD-114

To examine the antiviral activity of Tetherin/BST-2, 293T cells (2×10^5) were cotransfected with pTERD-114 (100 ng) and either pTeth-FL or pfelTeth-FL (25, 50, 100, or 200 ng) using Trans-IT LT-1 (Mirus Bio Corp., Madison, WI). Forty-eight hours after transfection, virion-containing culture supernatants were clarified by centrifugation (10,000×*g*; 15 min) and virions were pelleted through a 16.5% sucrose cushion by ultracentrifugation (348,000×*g*; 40 min at 4°C). Cells were lysed with lysis buffer A [25]. Virion- and cell-associated proteins were analyzed by Western blotting using anti-RD-114 Gag antibody, anti-FLAG M2 antibody (Sigma), and anti-actin antibody (Sigma) as described previously [6,24]. The intensities of the bands for virion- and cell-associated Gag were quantified using a Fuji LAS3000 imaging system (Fuji Film, Tokyo, Japan). The control vector (virus $p28^{CA}$/virus $p28^{CA}$ + cellular $p28^{CA}$ + $p68^{Gag}$) was set to 100%. Virus production was also examined by real-time RT-PCR. Viral RNAs were extracted from pelleted virions using a QIAamp Viral RNA Mini Kit (Qiagen). After DNaseI treatment, real-time RT-PCR was performed using the previously described primers targeting the RD-114 *pol* region [26]. Amplification was performed as described above.

Results

Cloning and sequence analysis of feline Tetherin/BST-2

Molecular cloning of complete coding region of feline Tetherin/BST-2 was carried out by RT-PCR and 5′-RACE using RNA extracted from three kinds of feline cell lines, CRFK, FL74, and QN10S cells, treated with IFN. The amino acid sequences of Tetherin/BST-2 from CRFK and FL74 cells were completely identical, while that from QN10S cells was different from those from CRFK and FL74 cells at three positions, 59, 80, and 116 (Figure 1). The nucleotide sequence of the coding region of feline Tetherin/BST-2 and the corresponding protein sequence have been deposited in DDBJ (AB564550). Furthermore, Figure 1 shows the amino acid sequence alignment of Tetherin/BST-2 from cat, dog (GenBank XM_860510), pig (GenBank NM_001161755), mouse (GenBank NM_198095), and human (GenBank NM_004335). The degree of sequence identity between feline Tetherin/BST-2 and those of dog, pig, mouse, and human were 57.7%, 48.7%, 42.5%, and 44.4%, respectively. Three cysteine residues in the extracellular domain, which appear to be important for dimer formation, are conserved among all species. Two putative *N*-linked glycosylation sites are conserved at the same positions among all species other than cat. The glycosylation site in the central region of extracellular domain, N79, is conserved in feline Tetherin/BST-2, while another glycosylation site, N119, is present in the relatively C-terminal region of the extracellular domain of feline Tetherin/BST-2, but not in the region close to the transmembrane domain as in other species. We also found that the N-terminal cytoplasmic tail of feline Tetherin/BST-2 is shorter than those of other species.

Induction of feline Tetherin/BST-2 in feline cells by IFN

It has been reported that human Tetherin/BST-2 is inducible by type I IFN [1,12]. To investigate whether the expression of feline Tetherin/BST-2 is induced by type I IFN, we treated CRFK cells with 100 or 1,000 units/ml of IFN-α A/D for 24 h and determined the level of feline Tetherin/BST-2 mRNA by quantitative real-time RT-PCR. Treatment with 100 or 1,000 units/ml of IFN-α induced increases of 75- and 320-fold in feline Tetherin/BST-2 mRNA level, respectively, compared to untreated cells (Figure 2A). CRFK cells constitutively express infectious endogenous retrovirus, RD-114. IFN treatment reduced RD-114 release from CRFK cells with a concomitant increase in feline Tetherin/BST-2 expression (Figure 2B), suggesting that feline Tetherin/BST-2 inhibits release of RD-114 virus particles from cells.

Antiviral activity of feline Tetherin/BST-2 against RD-114

To directly examine whether feline Tetherin/BST-2 has inhibitory activity against RD-114 virus release, the expression plasmid for feline Tetherin/BST-2 originated from CRFK cells or human Tetherin/BST-2 was cotransfected with the RD-114 infectious clone into 293T cells and RD-114 production was analyzed by Western blotting and real-time RT-PCR assay. As shown in Figure 3A, dose-dependent reductions in RD-114 release were observed with increasing expression levels of human and feline Tetherin/BST-2. Quantitative analyses of the amounts of RD-114 virions released from cells were also carried out by Western blotting and real-time RT-PCR assay (Figure 3B and C). The inhibition of RD-114 virus release by feline Tetherin/BST-2 was demonstrated by both Western blotting and real-time RT-PCR assay. Antiviral activity of feline Tetherin/BST-2 against

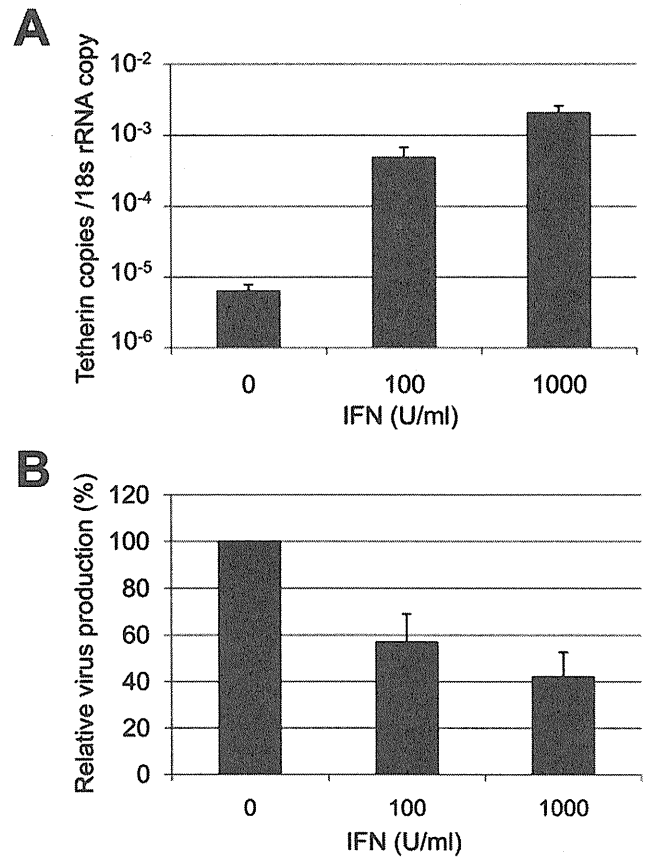

Figure 2. Induction of Tetherin/BST-2 and reduction of RD-114 particle release by IFN treatment of feline cells. CRFK cells were treated with 100 or 1,000 U/ml of IFN-α for 24 h. (A) feline Tetherin/BST-2 mRNA and 18S rRNA were quantified by real-time RT-PCR. The numbers of feline Tetherin/BST-2 mRNA copies were normalized to one copy of 18S rRNA. Histograms represent the averages from three independent experiments (± standard deviation of the mean). (B) RD-114 viral RNA in the supernatant from IFN-treated or untreated CRFK cells were quantified by real-time RT-PCR.
doi:10.1371/journal.pone.0018247.g002

RD-114 release was slightly weaker than that of human Tetherin/BST-2, although feline and human Tetherin/BST-2 were expressed at similar levels in cells transfected with the same amounts of each expression plasmid. We also confirmed that feline Tetherin/BST-2 originated from QN10S cells inhibits RD-114 production at the similar level to feline Tetherin/BST-2 originated from CRFK cells (data not shown).

Importance of *N*-linked glycosylation for antiviral activity

To examine the role of *N*-linked glycosylation of feline Tetherin/BST-2 in its antiviral function, we analyzed the effects of exogenous expression of mutants with a single or multiple mutations in the *N*-linked glycosylation sites (N79A, N119A, and N79A/N119A) on RD-114 production. 293T cells were cotransfected with the RD-114 infectious clone and increasing amounts of the expression plasmid for wild-type or mutant feline Tetherin/BST-2. Wild-type feline Tetherin/BST-2 was detected as triplet bands, while N79A and N119A mutants and N79A/N119A mutant showed double and single band(s), respectively (Figure 4), indicating that the upper, middle, and lower bands of triplet forms corresponded to multiple-, single-, and non-glycosylated forms, respectively. Exogenous expression of the N119A mutant significantly reduced RD-114 virus release as well as wild-type, while the inhibitory activity of the N79A mutant on the RD-114 virus release was lower than those of wild-type and N119A mutant despite the much higher expression level (Figure 4). Furthermore, the N79A/N119A mutant without glycosylation almost completely lost its antiviral activity. In addition, the antiviral activity of the N79A/N119A mutant could not be overcome by increased expression. These results indicated that glycosylation at N119 is not essential for the antiviral activity of feline Tetherin/BST-2, while the loss of glycosylation at N79 or at both N79 and N119 markedly affected its antiviral activity.

Feline Tetherin/BST-2 is insensitive to antagonism by HIV-1 Vpu

HIV-1 Vpu has been shown to antagonize the antiviral activity of human Tetherin/BST-2, but not monkey Tetherin/BST-2. To examine the sensitivity of feline Tetherin/BST-2 to Vpu, pVpu-Myc, which expresses Vpu containing a Myc-tag at the N-terminus, was cotransfected into 293T cells along with the RD-114 infectious clone and the expression plasmid for human or feline Tetherin/BST-2. RD-114 production was analyzed by Western blotting. As expected, Vpu expression partially rescued the RD-114 release reduction by human Tetherin/BST-2, but not that by feline Tetherin/BST-2 (Figure 5), indicating that Vpu has no effect on the antiviral activity of feline Tetherin/BST-2.

Discussion

In this study, we identified feline Tetherin/BST-2 and demonstrated the antiviral activity of feline Tetherin/BST-2.

The degree of sequence identity between feline Tetherin/BST-2 and those of dog, pig, mouse, and human were 57.7%, 48.7%, 42.5%, and 44.4%, respectively. As compared to the other cellular antiviral factors including APOBEC3 and TRIM5 proteins, the sequence homologies of Tetherin/BST-2 among mammalian species are relatively low. It has been reported that the antiviral activity of Tetherin/BST-2 require the structural features such as an N-terminal transmembrane region, a C-terminal GPI anchor, and a proper

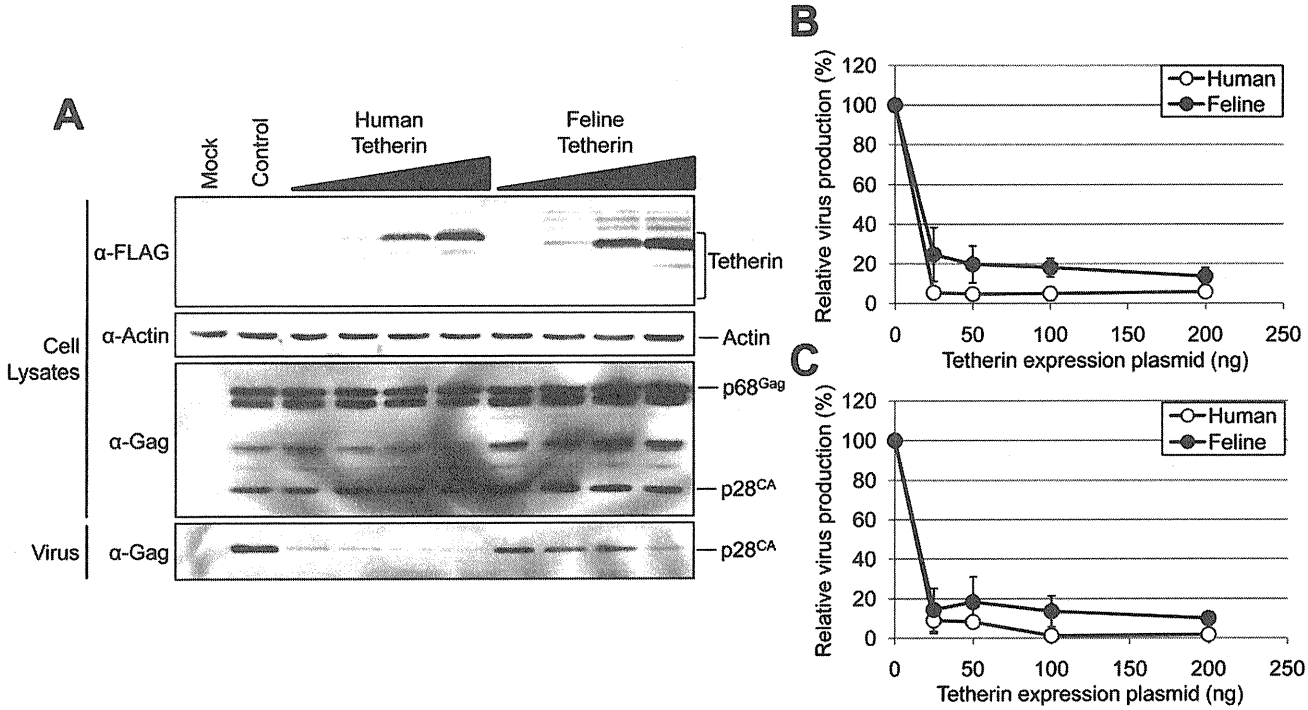

Figure 3. Inhibition of RD-114 particle release by feline Tetherin/BST-2. Both RD-114 vector (100 ng) and the expression vector for human or feline Tetherin/BST-2 containing FLAG-tag (25, 50, 100, or 200 ng) were cotransfected into 293T cells. Cells and viruses were collected at 48 h after transfection, and analyzed by Western blotting (A). The intensities of the bands for virus- and cell-associated Gag were quantified using a Fuji LAS3000 imaging system (Fuji Film) (B). The control vector (virus $p28^{CA}$/virus $p28^{CA}$ + cellular $p28^{CA}$ + $p68^{Gag}$) was set to 100%. Histograms represent the averages from three independent experiments (± standard deviation of the mean). (C) RD-114 viral RNA in the supernatant from cells was quantified by real-time RT-PCR.
doi:10.1371/journal.pone.0018247.g003

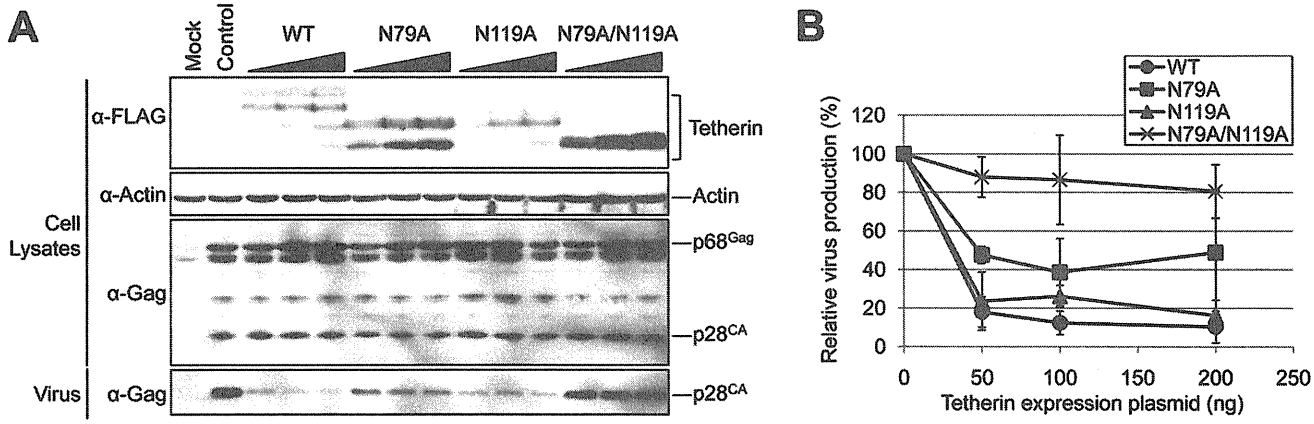

Figure 4. Importance of *N*-linked glycosylation for the antiviral activity. Both RD-114 vector (100 ng) and the expression vector for wild-type or mutant feline Tetherin/BST-2 (50, 100, or 200 ng) were cotransfected into 293T cells. Cells and viruses were collected at 48 h after transfection, and analyzed by Western blotting (A). The intensities of the bands for virus and cell-associated Gag were quantified using a Fuji LAS3000 imaging system (B). The control vector (virus $p28^{CA}$/virus $p28^{CA}$ + cellular $p28^{CA}$ + $p68^{Gag}$) was set to 100%. Histograms represent the averages from three independent experiments (± standard deviation of the mean).
doi:10.1371/journal.pone.0018247.g004

coiled-coil formation of extracellular region, but not exact amino acid sequences [11]. It would be the reason why the sequence homologies of Tetherin/BST-2 among mammalian species are relatively low.

As expected, we found that feline Tetherin/BST-2 efficiently inhibited the release of feline endogenous retrovirus RD-114 from cells, although the inhibitory effect of feline Tetherin/BST-2 against RD-114 release was slightly weaker than that of human Tetherin/BST-2 (Figure 3). RD-114 has been reported to be produced as infectious viruses in some feline cell lines and to be present as a contaminant in a proportion of live attenuated vaccines for pets [21]. It is very difficult to completely exclude the proviral DNA of RD-114 from cells, as endogenous retroviruses are usually integrated into multiple loci of the host chromosomes. The induction or exogenous expression of feline Tetherin/BST-2 in these feline cells may be useful as a novel strategy to reduce the risk of the RD-114 contamination into vaccines or biological products.

The sequence analysis of feline Tetherin/BST-2 showed that the N-terminus of feline Tetherin/BST-2 was shorter than those of other species (Figure 1). It has been reported that a dual-tyrosine motif ($Y\text{-}Y_{6-8}$) in the cytoplasmic domain of human Tetherin/BST-2 is crucial for clathrin-mediated endocytosis through recruiting AP-1 and AP-2 adaptor proteins [27,28]. Feline Tetherin/BST-2 may be internalized *via* a different pathway from the others, since feline Tetherin/BST-2 does not have this dual-tyrosine motif in its cytoplasmic domain. These features may have an effect on the weaker antiviral activity of feline Tetherin/BST-2 compared to human Tetherin/BST-2. However, at present, it is not clear whether the short cytoplasmic domain and deficiency of the dual-tyrosine motif are involved in any function of feline Tetherin/BST-2.

Although the expression levels of N79A and N79A/N119A mutants in cells were much higher than those of wild-type and N119A, the loss of glycosylation at N79, but not N119, reduced the antiviral activity of feline Tetherin/BST-2 (Figure 4). Moreover, the loss of glycosylation at both N79 and N119 almost completely inactivated the antiviral activity against RD-114. Glycosylation at N79 is conserved among Tetherin/BST-2 homologs from many species including cat (Figure 1), suggesting that this glycosylation plays an important role in the structure and function of this molecule. In addition, it has been reported previously that *N*-linked glycosylation at the corresponding site of human Tetherin/BST-2 is important for antiviral activity against HIV-1 [11]. On the other hand, glycosylation at N119 is unique in feline Tetherin/BST-2 and appears to be dispensable for the antiviral activity. Although it is not clear how glycosylation of Tetherin/BST-2 affect its antiviral activity, it has been reported that the cell surface expression levels of the glycosylation mutants of human Tetherin/BST-2 are less than that of WT [11]. The lacking of glycosylation signal may affect the intracellular transport of Tetherin/BST-2 and result in loss of the antiviral activity of Tetherin/BST-2.

HIV-1 Vpu has been reported to recognize several amino acid residues in the transmembrane domain of human Tetherin/BST-2

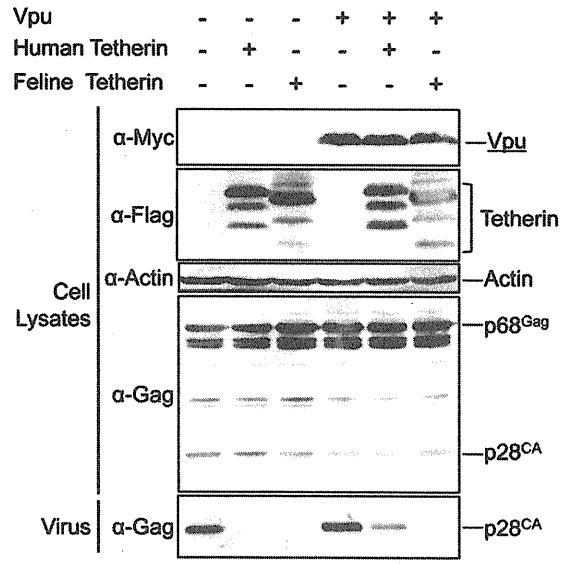

Figure 5. Feline Tetherin/BST-2 is insensitive to antagonism by HIV-1 Vpu. Both RD-114 vector (100 ng) and the expression vector for human or feline Tetherin/BST-2 containing FLAG-tag (200 ng), with or without the expression vector for Vpu containing Myc-tag (1 μg), were cotransfected into 293T cells. Cells and viruses were collected at 48 h after transfection, and analyzed by Western blotting.
doi:10.1371/journal.pone.0018247.g005

and antagonize the antiviral activity of human Tetherin/BST-2 [29,30,31]. The activity of Vpu as a Tetherin/BST-2 antagonist appears to be species specific, since Vpu inhibits the antiviral activity of human Tetherin/BST-2, but not monkey Tetherin/BST-2. In this study, we demonstrated that Vpu inhibited the reduction of RD-114 virus release by human Tetherin/BST-2, but not feline Tetherin/BST-2 (Figure 5). In addition, the cytoplasmic domain of feline Tetherin/BST-2 does not have the STS motif (at position 3-5) required for Vpu/β-TrCP-dependent ubiquitination [32]. Thus, our data support that the activity of Vpu as a Tetherin/BST-2 antagonist is specific for human Tetherin/BST-2.

Similar to human Tetherin/BST-2, the feline homolog is likely to also have antiviral activity against not only RD-114 but also a wide variety of enveloped viruses, although we demonstrated the antiviral activity of feline Tetherin/BST-2 against RD-114. In addition, we showed that the expression of feline Tetherin/BST-2 was induced by type I IFN similar to human Tetherin/BST-2 (Figure 2), suggesting that Tetherin/BST-2 functions as a host innate antiviral system against a wide variety of viruses. Analyses of the expression pattern of feline Tetherin/BST-2 *in vivo* and the mechanism of induction of Tetherin/BST-2 by IFN would be useful for understanding the specificity (tropism) of virus replication in tissues or cells and the development of antiviral strategies against a wide variety of viruses.

Acknowledgments

We thank Toshie Sakuma for plasmid preparation.

Author Contributions

Conceived and designed the experiments: AF MA YM TM JY. Performed the experiments: AF JY. Analyzed the data: AF TM YM JY. Contributed reagents/materials/analysis tools: AF MA TM JY. Wrote the paper: AF JY.

References

1. Neil SJD, Zang T, Bieniasz PD (2008) Tetherin inhibits retrovirus release and is antagonized by HIV-1 Vpu. Nature 451: 425–U421.
2. Jouvenet N, Neil SJ, Zhadina M, Zang T, Kratovac Z, et al. (2009) Broad-spectrum inhibition of retroviral and filoviral particle release by tetherin. J Virol 83: 1837–1844.
3. Mattiuzzo G, Ivol S, Takeuchi Y (2010) Regulation of porcine endogenous retrovirus release by porcine and human tetherins. J Virol 84: 2618–22.
4. Göttlinger HG, Dorfman T, Cohen EA, Haseltine WA (1993) Vpu protein of human immunodeficiency virus type 1 enhances the release of capsids produced by gag gene constructs of widely divergent retroviruses. Proc Natl Acad Sci USA 90: 7381–7385.
5. Kaletsky RL, Francica JR, Agrawal-Gamse C, Bates P (2009) Tetherin-mediated restriction of filovirus budding is antagonized by the Ebola glycoprotein. Proc Natl Acad Sci USA 106: 2886–2891.
6. Sakuma T, Noda T, Urata S, Kawaoka Y, Yasuda J (2009) Inhibition of Lassa and Marburg virus production by tetherin. J Virol 83: 2382–2385.
7. Mansouri M, Viswanathan K, Douglas JL, Hines J, Gustin J, et al. (2009) Molecular mechanism of BST2/tetherin downregulation by K5/MIR2 of Kaposi's sarcoma-associated herpesvirus. J Virol 83: 9672–9681.
8. Kupzig S, Korolchuk V, Rollason R, Sugden A, Wilde A, et al. (2003) Bst-2/HM1.24 is a raft-associated apical membrane protein with an unusual topology. Traffic 4: 694–709.
9. Ohtomo T, Sugamata Y, Ozaki Y, Ono K, Yoshimura Y, et al. (1999) Molecular cloning and characterization of a surface antigen preferentially overexpressed on multiple myeloma cells. Biochem Biophys Res Commun 258: 583–591.
10. Andrew AJ, Miyagi E, Kao S, Strebel K (2009) The formation of cysteine-linked dimers of BST-2/tetherin is important for inhibition of HIV-1 virus release but not for sensitivity to Vpu. Retrovirology. 6: 80.
11. Perez-Caballero D, Zang T, Ebrahimi A, McNatt MW, Gregory DA, et al. (2009) Tetherin inhibits HIV-1 release by directly tethering virions to cells. Cell 139: 499–511.
12. Blasius AL, Giurisato E, Cella M, Schreiber RD, Shaw AS, et al. (2006) Bone marrow stromal cell antigen 2 is a specific marker of type I IFN-producing cells in the naive mouse, but a promiscuous cell surface antigen following IFN stimulation. J Immunol 177: 3260–3265.
13. Ishikawa J, Kaisho T, Tomizawa H, Lee BO, Kobune Y, et al. (1995) Molecular cloning and chromosomal mapping of a bone marrow stromal cell surface gene, BST2, that may be involved in pre-B-cell growth. Genomics 26: 527–534.
14. Le Tortorec A, Neil SJD (2009) Antagonism to and intracellular sequestration of human tetherin by the human immunodeficiency virus type 2 envelope glycoprotein. J Virol 83: 11966–11978.
15. Zhang F, Wilson SJ, Landford WC, Virgen B, Gregory D, et al. (2009) Nef proteins from simian immunodeficiency viruses are tetherin antagonists. Cell Host Microbe 6: 54–67.
16. Sauter D, Schindler M, Specht A, Landford WN, Münch J, et al. (2009) Tetherin-driven adaptation of Vpu and Nef function and the evolution of pandemic and nonpandemic HIV-1 strains. Cell Host Microbe 6: 409–421.
17. Douglas JL, Gustin JK, Viswanathan K, Mansouri M, Moses AV, et al. (2010) The great escape: viral strategies to counter BST-2/tetherin. PLoS Pathog 6: e1000913.
18. Reeves RH, Nash WG, O'Brien SJ (1985) Genetic mapping of endogenous RD-114 retroviral sequences of domestic cats. J Virol 56: 303–306.
19. Baumann JG, Gunzburg WH, Salmons B (1998) CrFK feline kidney cells produce an RD114-like endogenous virus that can package murine leukemia virus-based vectors. J Virol 72: 7685–7687.
20. Yoshikawa R, Sato E, Igarashi T, Miyazawa T (2010) Characterization of RD-114 virus isolated from a commercial canine vaccine manufactured using CRFK cells. J Clin Microbiol 48: 3366–3369.
21. Miyazawa T, Yoshikawa R, Golder M, Okada M, Stewart H, et al. (2010) Isolation of an infectious endogenous retrovirus in a proportion of live attenuated vaccines for pets. J Viol 84: 3690–3694.
22. Dunn KJ, Yuan CC, Blair DG (1993) A phenotypic host range alteration determines RD114 virus restriction in feline embryonic cells. J Virol 67: 4704–4711.
23. Urata S, Noda T, Kawaoka Y, Yokosawa H, Yasuda J (2006) Cellular factors required for Lassa virus budding. J Virol 80: 4191–4195.
24. Sakuma T, Sakurai A, Yasuda J (2009) Dimerization of tetherin is not essential for its antiviral activity against Lassa and Marburg viruses. PLoS ONE 4: e6934.
25. Yasuda J, Hunter E (1998) A proline-rich motif (PPPY) in the Gag polyprotein of Mason-Pfizer monkey virus plays a maturation-independent role in virion release. J Virol 72: 4095–4103.
26. Sakaguchi S, Okada M, Shojima T, Baba K, Miyazawa T (2008) Establishment of a LacZ marker rescue assay to detect infectious RD114 virus. J Vet Med Sci 70: 785–790.
27. Rollason R, Korolchuk V, Hamilton C, Schu P, Banting G (2007) Clathrinmediated endocytosis of a lipid-raft-associated protein is mediated through a dual tyrosine motif. J Cell Sci 120: 3850–3858.
28. Masuyama N, Kuronita T, Tanaka R, Muto T, Hirota Y, et al. (2009) HM1.24 is internalized from lipid rafts by clathrin-mediated endocytosis through interaction with alpha-adaptin. J Biol Chem 284: 15927–15941.
29. Gupta RK, Hué S, Schaller T, Verschoor E, Pillay D, et al. (2009) Mutation of a single residue renders human tetherin resistant to HIV-1 Vpu-mediated depletion. PLoS Pathog 5: e1000443.
30. McNatt MW, Zang T, Hatziioannou T, Bartlett M, Fofana IB, et al. (2009) Species-specific activity of HIV-1 Vpu and positive selection of tetherin transmembrane domain variants. PLoS Pathog 5: e1000300.
31. Rong L, Zhang J, Lu J, Pan Q, Lorgeoux RP, et al. (2009) The transmembrane domain of BST-2 determines its sensitivity to down-modulation by human immunodeficiency virus type 1 Vpu. J Virol 83: 7536–7546.
32. Tokarev AA, Munguia J, Guatelli JC (2010) Serine-threonine ubiquitination mediates downregulation of BST-2/tetherin and relief of restricted virion release by HIV-1 Vpu. J Virol 85: 51–63.

ANTIMICROBIAL AGENTS AND CHEMOTHERAPY, Sept. 2011, p. 4251–4260 Vol. 55, No. 9
0066-4804/11/$12.00 doi:10.1128/AAC.00299-11

Novel Postentry Inhibitor of Human Immunodeficiency Virus Type 1 Replication Screened by Yeast Membrane-Associated Two-Hybrid System▽

Emiko Urano,[1,2] Noriko Kuramochi,[3] Reiko Ichikawa,[2] Somay Yamagata Murayama,[1] Kosuke Miyauchi,[2] Hiroshi Tomoda,[3] Yutaka Takebe,[2] Milan Nermut,[4] Jun Komano,[2]* and Yuko Morikawa[1]*

Kitasato Institute for Life Sciences and Graduate School of Infection Control, Kitasato University, Shirokane 5-9-1, Minato-ku, Tokyo 108-8641, Japan[1]; AIDS Research Center, National Institute of Infectious Diseases, Toyama 1-23-1, Shinjuku-ku, Tokyo 162-8640, Japan[2]; Faculty of Pharmaceutical Sciences, Kitasato University, Shirokane 5-9-1, Minato-ku, Tokyo 108-8641, Japan[3]; and National Institute for Biological Standards and Control, South Mimms, Herts EN6 3QG, United Kingdom[4]

Received 3 March 2011/Returned for modification 25 April 2011/Accepted 1 July 2011

Human immunodeficiency virus (HIV) Gag protein targets to the plasma membrane and assembles into viral particles. In the next round of infection, the mature Gag capsids disassemble during viral entry. Thus, Gag plays a central role in the HIV life cycle. Using a yeast membrane-associated two-hybrid assay based on the SOS-RAS signaling system, we developed a system to measure the Gag-Gag interaction and isolated 6 candidates for Gag assembly inhibitors from a chemical library composed of 20,000 small molecules. When tested in the human MT-4 cell line and primary peripheral blood mononuclear cells, one of the candidates, 2-(benzothiazol-2-ylmethylthio)-4-methylpyrimidine (BMMP), displayed an inhibitory effect on HIV replication, although a considerably high dose was required. Unexpectedly, neither particle production nor maturation was inhibited by BMMP. Confocal microscopy confirmed that BMMP did not block Gag plasma membrane targeting. Single-round infection assays with envelope-pseudotyped and luciferase-expressing viruses revealed that BMMP inhibited HIV replication postentry but not simian immunodeficiency virus (SIV) or murine leukemia virus infection. Studies with HIV/SIV Gag chimeras indicated that the Gag capsid (CA) domain was responsible for the BMMP-mediated HIV postentry block. *In vitro* studies indicated that BMMP accelerated disassembly of HIV cores and, conversely, inhibited assembly of purified CA protein in a dose-dependent manner. Collectively, our data suggest that BMMP primarily targets the HIV CA domain and disrupts viral infection postentry, possibly through inducing premature disassembly of HIV cores. We suggest that BMMP is a potential lead compound to develop antiretroviral drugs bearing novel mechanisms of action.

Over 2 decades, research has developed antiretroviral therapy (ART) with a combination of antiretroviral drugs for human immunodeficiency virus type 1 (HIV-1) infection (10). ART has dramatically improved the survival of HIV-1-infected individuals. Current ART involves a combination of inhibitors of HIV-specific enzymes, such as protease (PR), reverse transcriptase (RT), and integrase (IN). In some cases, inhibitors of HIV-1 entry are also used. However, the emergence of HIV-1 variants resistant to antiretroviral drugs during ART stresses the need for novel HIV-1 inhibitors against distinct targets.

Multiple screening approaches have been employed for HIV-1 drug discovery (37) and have successfully discovered HIV-1 inhibitors that are currently available: nucleoside analogue RT inhibitors were discovered by HIV replication assays (23) and PR inhibitors were produced by structure-based drug design (25). In general, cell-free assays allow discovery of compounds with a relatively low 50% effective dose (ED_{50}) *in vitro*. However, many such compounds often fail to inhibit HIV-1 replication in *in vivo* assays, because they may not penetrate the cell membrane or may easily be catalyzed in metabolic environments. Also, possible toxic effects of the compounds must be tested in a subsequent cell culture study. In contrast, cell-based screens can exclude toxic compounds but have the disadvantages of time requirements and limitations on cell propagation in high-throughput screening.

Recently, cell-based assays using engineered cells and microorganisms have become an attractive alternative to *in vitro* assays for high-throughput screening. The yeast *Saccharomyces cerevisiae* is a convenient alternative to mammalian cells for this purpose. Comparative genomic analysis has shown that approximately 30% of yeast genes have homology to the mammalian protein sequences (8), indicating that basic cellular mechanisms are well conserved between yeast and human cells. Yeast has been used as a model organism for understanding biological functions of higher eukaryotic cells, leading to accumulation of scientific knowledge in yeast genetics and molecular biology. Such pioneering research has allowed the development of molecular technologies (e.g., two-hybrid assay and galactose induction), genetically modified cells (e.g., temperature sensitivity and conditional lethality), and cell selection systems (e.g.,

* Corresponding author. Mailing address for Jun Komano: AIDS Research Center, National Institute of Infectious Diseases, Toyama 1-23-1, Shinjuku-ku, Tokyo 162-8640, Japan. Phone: 81-3-5285-1111. Fax: 81-3-5282-5037. E-mail: ajkomano@nih.go.jp. Mailing address for Yuko Morikawa: Kitasato Institute for Life Sciences and Graduate School of Infection Control, Kitasato University, Shirokane 5-9-1, Minato-ku, Tokyo 108-8641, Japan. Phone: 81-3-3444-6161. Fax: 81-3-5791-6268. E-mail: morikawa@lisci.kitasato-u.ac.jp.

▽ Published ahead of print on 11 July 2011.

URA3 nutritional selection), enabling the construction of simple readout assay systems.

Gag protein, the main structural component of retrovirus, directs particle assembly. HIV Gag protein is synthesized as a precursor protein, p55, which is composed of matrix (MA), capsid (CA), nucleocapsid (NC), and p6 domains, and cotranslationally myristoylated at the N-terminal glycine. Concomitant with the N-terminal myristoylation, p55Gag is targeted to the plasma membrane and assembled into virus particles (13, 22). During particle release, Gag undergoes proteolytic processing to generate the CA domain that forms the mature capsid. In the next round of infection, the mature capsid disassembles during viral penetration into host cell cytoplasm. Thus, the capsid assembly and disassembly are reverse reactions during virus release and entry and must be regulated by yet-unknown mechanisms. Indeed, the optimal stability of HIV-1 capsid is required for efficient infection (14). We have previously shown that the particle assembly process is reproducible in a yeast cell system (26). Here, we further developed a yeast membrane-associated two-hybrid assay system in which a temperature-sensitive mutant strain of yeast grows at restrictive temperature when Gag-Gag interactions occur. Using this yeast two-hybrid system, we have screened a chemical library composed of 20,000 low-molecular-weight compounds and have found a compound that targets CA-CA interactions and inhibits HIV-1 replication.

MATERIALS AND METHODS

Construction and transformation of yeast expression plasmids. A yeast membrane-associated two-hybrid assay based on the CytoTrap SOS recruitment system (Stratagene) was employed in this study. The full-length *gag* gene of HIV-1 (HXB2 strain) was placed downstream of the yeast inducible promoter for the *GAL1* gene in frame with the cDNA of SOS in a pSOS plasmid (Stratagene) that contains the *LEU2* gene as a yeast selective marker. The HIV-1 (HXB2 strain) *gag* gene was also cloned into pMyr plasmid, which contains a yeast inducible promoter for the *GAL1* gene and the *URA3* gene as a selective marker. The *S. cerevisiae* strain cdc25Ha (*MATa ura3-52 his3-200 ade2-101 lys2-801 trp1-901 leu2-3 112 cdc25-2* Gal^+) was doubly transformed with the yeast expression plasmids.

Chemical library screening in CytoTrap yeast membrane-associated two-hybrid system. Yeast transformants were initially grown at 25°C in synthetic defined medium with glucose (0.67% yeast nitrogen base, 2% glucose, and amino acid mixtures without uracil or leucine) (permissive conditions). After being washed, culture was diluted to an optical density at 600 nm (OD_{600}) of 0.1 in synthetic defined medium with galactose and raffinose (0.67% yeast nitrogen base, 2% galactose, 2% raffinose, and amino acid mixtures without uracil or leucine) for Gag expression. The yeast culture (OD_{600} = 0.1) was incubated with a chemical library (a final concentration of 10 μM) at 37°C for 5 days (restrictive conditions) in 96-well microtiter plates with shaking. The chemical library (preplated Diversity Set) was purchased from Enamine. After complete resuspension of cells by vortexing of microtiter plates, cell density was measured at 600 nm by a plate reader (Infinite200; Tecan).

Mammalian cells and transfection. 293T, HeLa, and MT-4 cells were provided by the AIDS Research Center, National Institute of Infectious Diseases, Japan. 293FT cells were purchased from Invitrogen. Peripheral blood monocytic cells (PBMC) were isolated by Ficoll-Conray density centrifugation from healthy donors. All mammalian cells were maintained in RPMI 1640 medium (Sigma) supplemented with 10% fetal bovine serum (Japan Bioserum, Japan), 100 U/ml penicillin, and 100 mg/ml streptomycin (Invitrogen), at 37°C in a humidified 5% CO_2 atmosphere. For PBMC culture, GlutaMax-I (Invitrogen), insulin-transferrin-selenium A (Invitrogen), 200 ng/ml anti-CD3 monoclonal antibody (OKT3; Janssen Pharmaceutical), and 70 U/ml recombinant human interleukin-2 (IL-2; Shionogi Pharmaceutical, Japan) were further added to the medium. Transfection was carried out with Lipofectamine 2000 according to the manufacturer's protocol (Invitrogen).

Cell toxicity assays. For determining the toxicity of the chemical library to yeast, yeast cultures were diluted to an OD_{600} of 0.01 and incubated under permissive conditions (at 25°C in glucose medium) with the chemical library. After 2 days, cell density was measured at 600 nm by a plate reader (Infinite200; Tecan). For determining toxicity to mammalian cells, 293T, 293FT, HeLa, and MT-4 cells and PBMC were incubated with compounds at 37°C for 2 to 14 days and subjected to 3-(4,5-dimethylthiazol-2-yl)-5-(3-carboxymethoxyphenyl)-2-(4-sulfophenyl)-2H-tetrazolium (MTS) and Alamar Blue assays according to the manufacturer's instructions. The OD of the MTS assay mixture was measured at 490 nm, and the OD of the Alamar Blue assay mixture was measured at 570 nm by a plate reader (FLx800; BioTek). The 50% cytotoxicity concentrations were defined as drug concentrations by which the OD values reached the 50% level of the no-drug (dimethyl sulfoxide [DMSO]) controls.

HIV-1 replication assays. MT-4 Luc cells that were transduced with luciferase in MT-4 cells (31) and PBMC were grown in RPMI 1640 medium supplemented with 10% fetal bovine serum. MT-4 Luc cells were infected with HIV-1 (HXB2 strain) corresponding to 1.25 ng of p24CA antigen and incubated at 37°C in the presence of compounds. On day 7, MT-4 Luc cells were subjected to luciferase assay. PBMC were stimulated with IL-2 and anti-CD3 antibody. Following infection with HIV-1 (HXB2 strain) corresponding to approximately 5 ng of p24CA antigen, PBMC were incubated at 37°C and passaged every 3 to 4 days in the presence of compounds. The culture supernatants of PBMC were temporally collected and subjected to quantification of HIV-1 particle yields by p24CA antigen capture enzyme-linked immunosorbent assay (ELISA; Zeptometrix).

Single-round infection assays. For single-round infection assays, HIV-1 was pseudotyped with either HIV-1 Env protein or vesicular stomatitis virus (VSV) G protein as described previously (35). Briefly, 293FT cells were transfected with a plasmid containing the codon-optimized HXB2 *gag-pol* gene (pHIVgag-pol), a lentiviral plasmid expressing luciferase (pLenti-luciferase), a plasmid expressing HIV-1 Rev (pRevpac), and either a plasmid expressing HIV-1 Env or a plasmid expressing VSV-G. Culture media were harvested and inoculated into MT-4 and 293FT cells in the presence of 5 to 10 μg/ml dextran (ICN). HIV-1 pseudotyped with autologous HIV-1 Env protein was inoculated into 293FT-CD4 (expressing CD4 constitutively) cells. On day 2 or 3, infectivity was assessed by luciferase activity transduced by pLenti-luciferase. HIV-1 (NL43 strain) expressing luciferase, simian immunodeficiency virus (SIV) (mac239 strain), and murine leukemia virus (MLV) (Moloney strain) were similarly pseudotyped with VSV-G (28). The viruses were enriched by centrifugation through sucrose cushions if necessary.

HIV/SIV Gag chimeras were generated in the context of pHIVgag-pol by replacing the MA and CA domains with the SIV MA and CA domains, respectively. The Gag chimeras contain the cleavage site sequences of HIV-1 Gag at the chimera junctions. Amino acid substitutions G89A and P90A in the cyclophilin A (CypA)-binding loop of CA (corresponding to Gag amino acid positions 225 and 226) (11, 16) were carried out by overlap PCR in the context of pHIVgag-pol.

Quantitative PCR for HIV-1 cDNA synthesis. MT-4 cells were infected with HIV-1 (HXB2 strain) and incubated in the presence of compounds. Efavirenz (EFV) was provided by the NIH AIDS Research and Reference Reagent Program and was used as positive control. The cellular genomic DNA was extracted 4 and 24 h postinfection with a DNeasy kit (Qiagen) according to the manufacturer's instructions. The cellular DNA was subjected to quantitative real-time PCR using the Quantitec probe PCR kit containing SYBR green (Qiagen). The following primer sets were used: 5′-AACTAGGGAACCCACTGCTTAAG-3′ and 5′-CTGCTAGAGATTTTCCACACTGAC-3′ (specific for the R-U5 region in early reverse transcripts of HIV-1 cDNA), 5′-CCGTCTGTTGTGTGACTC TGGT-3′ and 5′-GAGTCCTGCGTCGAGAGAGCT-3′ (specific for the late reverse transcripts of HIV-1 cDNA), 5′-TGCTGGGATTACAGGCGTGAG-3′ and 5′-CTGCTAGAGATTTTCCACACTGAC-3′ (specific for long terminal repeat [LTR] and *Alu* region in the integrated HIV-1 cDNA), and 5′-AACTAG GGAACCCACTGCTTAAG-3′ and 5′-CTGCTAGAGATTTTCCACACTGA C-3′ (second PCR) (specific for LTR region in the integrated HIV-1 cDNA) (12). The amplification kinetics was monitored by the Opticon 2 system (Bio-Rad). The levels of cellular DNA were normalized by the levels of β-globin DNA quantified using primers 5′-TATTGGTCTCCTTAAACCTGTCTTG-3′ and 5′-CTGACACAACTGTGTTCACTAGC-3′ (19).

Viral protein expression and particle purification. HIV-1 proviral clone pHXB2 was transfected into 293FT and HeLa cells in the presence of increasing doses of 2-(benzothiazol-2-ylmethylthio)-4-methylpyrimidine (BMMP). After 2 days, cells were analyzed by Western blotting using anti-HIV-1 p24CA monoclonal antibody (100-fold diluent of 183-H12-5C hybridoma culture supernatant; NIH AIDS Research and Reference Reagent Program). HIV particles were collected by centrifugation through 20% (wt/vol) sucrose cushions in an SW55

rotor (Beckman Coulter) at 120,000 × *g* for 1 h. For HIV/SIV Gag chimeras, 293FT cells were cotransfected with pHIVgag-pol expressing Gag chimera, pLenti-luciferase, pRevpac, and a plasmid expressing VSV-G. Cells and purified particles were similarly analyzed by Western blotting using anti-HIV-1 p24CA, anti-HIV-1 p17MA (2 μg/ml; 13-103-100; Advanced Biotechologies), and anti-SIV p27CA (1 μg/ml; 4324; Advanced Bioscience Laboratories) monoclonal antibodies.

***In vitro* assembly reaction of CA.** The *in vitro* assembly reaction of CA was performed as described previously (17, 36). Briefly, the purified HIV-1 CA (a final concentration of 100 μM) was incubated at 37°C for 1 h in buffer containing 20 mM Tris (pH 8.0), 500 mM NaCl, 0.2 mM EDTA, and 1 mM dithiothreitol. Assembly products were pelleted by centrifugation at 18,000 × *g* for 30 min at 4°C and were subjected to p24CA antigen capture ELISA (Zeptometrix) and electron microscopy.

***In vitro* disassembly reaction of capsid cores.** The *in vitro* disassembly assay was performed according to Aiken's method with some modifications (3). HIV particles were purified by ultracentrifugation through 20% (wt/vol) sucrose cushions. For isolation of HIV capsid cores, purified HIV particles were applied onto sucrose step gradients composed of 7.5% (wt/vol), 15% (wt/vol) containing 1% Triton X-100, and 30 to 70% (wt/vol) sucrose and subjected to centrifugation at 120,000 × *g* for 16 h at 4°C. Fractions rich in HIV cores were collected and resuspended in buffer (10 mM Tris [pH 7.4], 100 mM NaCl, and 1 mM EDTA). For core disassembly assays, aliquots of HIV cores were incubated at 37°C in the presence of compounds. For comparison, azidothymidine (AZT) (Moravek Biochemicals) was added to the reaction mixture. Intact cores were recovered by centrifugation at 125,000 × *g* for 30 min at 4°C.

Confocal microscopy and electron microscopy. HeLa cells were transfected with a pNL43 derivative expressing Gag-green fluorescent protein (GFP) fusion protein but not *pol* gene products. Cells were fixed with 3.7% paraformaldehyde in phosphate-buffered saline (PBS) for 30 min at room temperature and were treated with 0.1% Triton X-100 for 10 min at room temperature for membrane permeabilization. Following nuclear staining with TO-PRO-3 (Molecular Probes), cells were mounted with antibleaching reagent and observed with a laser scanning microscope (TCS; Leica).

In vitro assembly products were adsorbed onto carbon-coated copper grids and stained with 2% (wt/vol) uranyl acetate. Sections were subjected to electron microscopy.

Statistical analysis. Intergroup comparisons were performed with paired *t* test (for parametric group analysis). All *P* values were considered significant if less than 0.05.

RESULTS

A yeast membrane-associated two-hybrid system for HIV-1 Gag-Gag interactions. For construction of a yeast cell-based Gag assembly system, we employed a yeast membrane-associated two-hybrid assay based on the CytoTrap SOS recruitment system (Stratagene) in this study (Fig. 1). For HIV-1 Gag expression, two yeast expression plasmids, pMyr and pSOS, were used: pMyr contains the yeast inducible promoter for the *GAL1* gene followed by a myristoylation signal (amino acid sequence, MGSSKSKPKDPSQRR) for membrane targeting and pSOS contains the constitutive promoter for the yeast *ADH* gene followed by the human SOS gene. The *gag* gene of HIV-1 (HXB2 strain) was cloned in frame with the myristoylation signal in pMyr. The *gag* gene was similarly cloned in frame with the SOS gene in pSOS that allowed production of SOS-Gag fusion protein (Fig. 1A). The *S. cerevisiae* cdc25H strain was doubly transformed with these Gag expression plasmids. The cdc25H strain contains a temperature-sensitive mutation in the CDC25 gene, which allows growth at 25°C (permissive temperature) but not at 37°C (restrictive temperature). SOS is the human orthologue of the yeast CDC25 and can activate the yeast RAS signal transduction pathway that complements the yeast *cdc25* defect (4). When myristoylated Gag and SOS-Gag are coexpressed in the cdc25H cells, the SOS-Gag is recruited to the plasma membrane through an interaction with the myristoylated Gag, leading to growth of the cdc25H cells at 37°C (Fig. 1B). We initially confirmed that the cdc25H cells transformed with the Gag/pMyr and Gag/pSOS plasmids grew at 37°C in galactose plus raffinose medium under conditions in which SOS-Gag fusion protein was expressed but not at 37°C in glucose medium under conditions in which SOS-Gag fusion was not expressed.

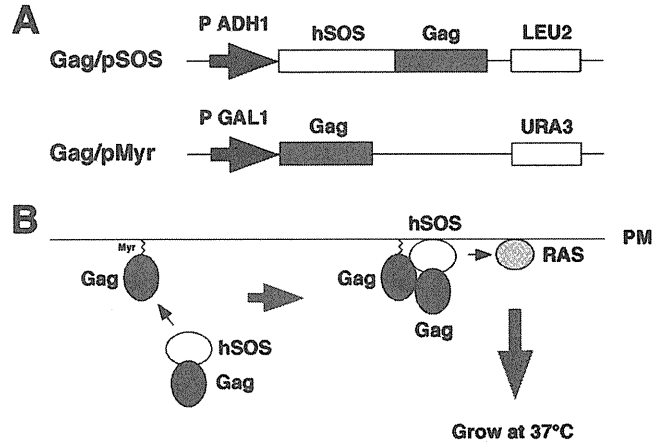

FIG. 1. Yeast membrane-associated two-hybrid screening for inhibitors of Gag-Gag interaction. (A) Schematic representation of Gag expression plasmids used for yeast SOS recruitment system. The full-length *gag* gene of HIV-1 (HXB2 strain) was expressed by yeast expression plasmids pMyr and pSOS: pMyr contains the yeast inducible promoter for the *GAL1* gene and the *URA3* gene as a selective marker and pSOS contains the constitutive promoter for the yeast *ADH* gene and the *LEU2* gene as a selective marker. (B) Principle of yeast membrane-associated two-hybrid assay based on SOS recruitment system. The schematic illustration was adapted with permission from the manuals for the CytoTrap yeast system (Agilent Technologies, Inc.; http://www.genomics.agilent.com/CollectionSubpage.aspx?PageType=Product&SubPageType=ProductDetail&PageID=1311).

Screening of a chemical library for Gag-Gag interaction inhibitors by yeast membrane-associated two-hybrid assays. For screening for inhibitors of Gag assembly, we optimized this yeast membrane-associated Gag-Gag interaction system to a liquid format using 96-well microplates. Using this system, we screened a chemical library composed of 20,000 compounds, each of which was initially designated by the numbers of microplates and wells of the chemical library (e.g., 172A6 indicates microplate number 172 and well number A6). When the cdc25H transformant was incubated at 37°C in galactose plus raffinose medium with a chemical library (10 μM each), we found 10 compounds that reduced cell growth (Fig. 2A, black columns). To examine if cell growth reduction is specifically due to the disruption of Gag-Gag interaction, we used another cdc25H transformant that contained MAFB/pSOS and SOS binding protein/pMyr plasmids. This combination produces SOS-MAFB fusion protein and myristoylated SOS binding protein and can be used as a positive control for the CytoTrap system (Stratagene). When using this positive control, we observed that 4 compounds (2G5, 73A7, 189A9, and 235C2) out of the 10 compounds also reduced cell growth (Fig. 2A, white columns), suggesting that they might inhibit pathways which are commonly used in the CytoTrap system (e.g., N myristoylation and RAS signaling). Thus, we concluded that 6 compounds (1G5, 31E7, 34A8, 73A5, 147B2, and 172A6) specifi-

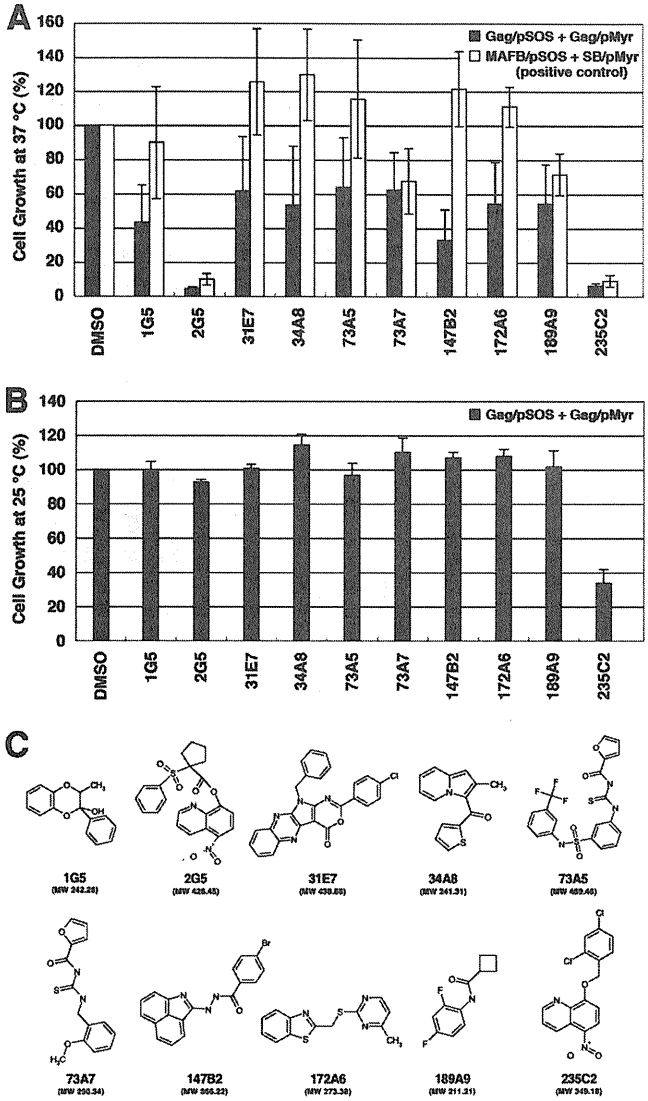

FIG. 2. Screening for inhibitors of Gag assembly by yeast membrane-associated two-hybrid assays. (A) The yeast cdc25Ha strain was transformed with the pSOS and pMyr plasmids. The yeast culture was diluted to an OD_{600} of 0.1 and incubated at 37°C in galactose-plus-raffinose medium (restrictive conditions) with a chemical library (a final concentration of 10 μM). After growth at 37°C for 5 days, cell density was measured at OD_{600}. As a control, the OD_{600} of yeast incubated in the presence of DMSO was set to 100%. The yeast transformed with the pSOS and pMyr plasmids, both of which contained the HIV-1 *gag* gene, was shown as black columns, and the yeast was transformed with the pSOS plasmid containing MAFB and the pMyr plasmid containing the cDNA of SB (as a positive-control combination) as white columns. Data were shown as means with standard deviations from 5 independent experiments. (B) The yeast cdc25Ha strain transformed with the pSOS and pMyr plasmids containing the HIV-1 *gag* gene was grown at 25°C in glucose medium. The yeast culture was diluted to an OD_{600} of 0.01 and incubated at 25°C in glucose medium with a chemical library (a final concentration of 10 μM). After growth at 25°C for 2 days, cell density was measured at OD_{600}. As a control, the OD_{600} of yeast incubated in the presence of DMSO was set to 100%. Data were shown as means with standard deviations from 3 independent experiments. (C) Structures of compounds screened from a chemical library by yeast membrane-associated two-hybrid assays.

cally inhibited a Gag-Gag interaction. No common chemical structures were found among the 6 candidates. However, 3 chemicals (34A8, 147B2, and 172A6) share relatively similar structures whereby two allyl groups are connected by a short linker moiety. To test the cell toxicity, the cdc25H transformants were incubated at 25°C in glucose medium (permissive conditions) with the compounds (10 μM each) (Fig. 2B). All the compounds except 235C2 allowed cell growth at levels comparable to that obtained in the presence of DMSO (as a control). Further studies revealed that 235C2 preferentially inhibited growth of several fungi *in vitro* (e.g., *Candida albicans* and *Aspergillus fumigatus* at MICs of 5.7 and 10 μM, respectively) (data not shown), suggesting that it might serve as a lead compound to develop an antifungal agent. The chemical formulas of 10 compounds are shown in Fig. 2C.

Inhibition of HIV replication in mammalian cells by compounds identified as yeast membrane-associated Gag-Gag interaction inhibitors. We evaluated the anti-HIV activity of the 6 candidates in mammalian cell systems. MT-4 Luc cells (human T lymphocytic cell line expressing luciferase constitutively) were infected with HIV-1 (HXB2 strain) and incubated at 37°C in the presence of the test compounds. In this T cell system, the luciferase activity is reduced by HIV-1 infection, due to the cell death upon HIV-1 replication (31). When added to HIV-1-infected MT-4 Luc cells, one of the candidates (172A6) recovered the luciferase expression in a dose-dependent manner (Fig. 3A), indicating that 172A6 was capable of reduction in HIV replication in mammalian cells. When 293T cells were incubated with the 6 compounds and were subjected to Alamar Blue assays, none of the compounds showed apparent reduction in cell viability (Fig. 3B). To confirm the anti-HIV effect, PBMC were infected with HIV-1 in the presence of 172A6 and production of HIV in the culture medium was temporally measured by p24CA antigen capture ELISA. 172A6 limited HIV replication at 5 μM and severely inhibited it at 25 μM (Fig. 3C, upper panel). When uninfected PBMC were similarly exposed to 172A6 and assessed by MTS assays, a slight reduction in cell viability was observed at 25 μM (Fig. 3C, lower panel). However, the severe inhibition of HIV replication at 25 μM 172A6 could not be ascribed fully to its cytotoxic effect. Using several mammalian cell lines, we reevaluated cytotoxicity of 172A6 by MTS assays. No significant cytotoxicity of 172A6 was seen in the cell lines, except in PBMC, that we used in this study (Fig. 3D). Based on the chemical structure [2-(benzothiazol-2-ylmethylthio)-4-methylpyrimidine] of the compound 172A6 (Fig. 2C), we called it BMMP here.

No inhibition of HIV particle release by BMMP. We initially examined whether BMMP inhibited HIV-1 particle production. 293FT cells were transfected with pHXB2 and incubated at 37°C in the presence of 5 to 50 μM BMMP. Western blotting using anti-HIV-1 p24CA antibody revealed that the intracellular level of Gag expression and the pattern of Gag processing were largely unaffected in the presence of BMMP (Fig. 4A), suggesting that BMMP did not inhibit HIV protease. When purified particle fractions were similarly analyzed, we found no reduction in particle production (Fig. 4A). We obtained similar results on HeLa cells. This indicates that BMMP did not block HIV-1 particle release.

Intracellular distribution of Gag was examined by confocal